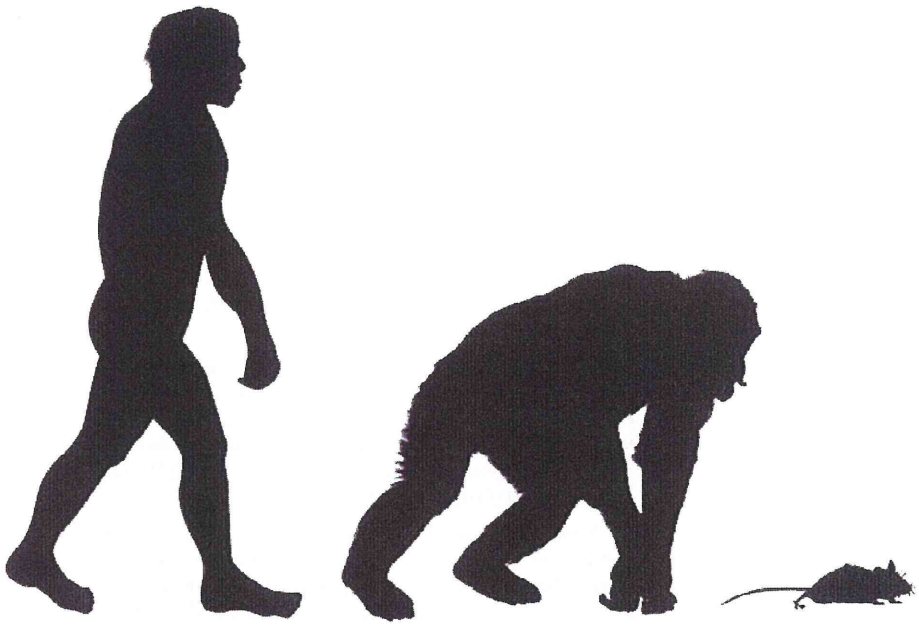

RESEARCH TECHNIQUE

The murine candidate

Small animals that mimic human hepatitis C infection will help researchers pinpoint weakness in the viral life cycle.

BY ELIE DOLGIN

The hepatitis C virus (HCV) is hard to study. Most of what researchers know about how it multiplies comes from cell-culture systems. Such cellular set-ups have proven invaluable for developing new drugs, including protease inhibitors and polymerase inhibitors, which prevent the virus from replicating its components inside the cell. Yet these cell-based systems fail to capture other important parts of the viral life cycle, such as the step before replication, when the virus attaches to liver cells and gains entry. What's more, cell-culture systems cannot reproduce the interaction between the immune system and the virus nor can they recapitulate entire organs so that liver pathology can be studied. For these reasons, researchers interested in how the virus causes disease have long sought a small-animal model.

Common laboratory animals, including rodents and most primates, are not susceptible hosts for HCV. Scientists have therefore had to settle for chimpanzees, which, like humans, are vulnerable to chronic HCV infections. However, "for ethical and economic reasons, the chimp is a terrible model," says Matthew Evans, an HCV researcher at the Mount Sinai School of Medicine in New York. Research involving chimpanzees is banned in many parts of the world, including Europe. And in most places where experimentation with great apes is allowed, laws against euthanizing chimps require investigators to fund the animals' long-term care — a prohibitively expensive commitment.

That's where a colony of ordinary-looking black mice running around in cages on the fourth floor of the Rockefeller University Comparative Bioscience Center in New York comes in. These animals might not look special, but they have been engineered to express either a pair or a quartet of human genes and, as such, are the first small animals with fully functioning immune systems that are prone to HCV infection. Using these models, "you can actually now look at hepatitis C virus entry *in vivo*," says Rockefeller immunologist Alexander Ploss, who developed the animals together with Charles Rice, executive and scientific director of the Center for the Study of Hepatitis C in New York.

NATURE.COM to read the latest research using animal models go.nature.com/qDGI2e

These mice, and others like them, could provide a cheaper, more robust and less ethically fraught route to HCV drug and vaccine discovery.

THE HUMAN SIDE

Getting to this point has been a hard slog. In the years immediately after the virus was first described in 1989, many research teams developed transgenic mice carrying one or more genes encoding HCV proteins. Thus it was possible to study HCV-induced liver pathology without infecting mice with the virus. This approach still has some proponents. Last year, a team led by Matti Sällberg, a viral immunologist at the Karolinska Institute in Stockholm, used mice expressing the viral protease and showed that treatment with a drug targeting the cytokine tumour-necrosis factor-α led to improved liver function[1].

But the approach is highly artificial, leading to overexpression of the introduced viral genes and ignoring the rest of the viral life cycle. Over the past decade, most researchers have moved away from this set-up in favour of systems that involve infecting animals with the virus.

The first such model was reported ten years ago by a team led by transplant surgeon Norman Kneteman at the University of Alberta, in Edmonton, Canada. Kneteman's group engineered mice to express a gene that kills off the animals' own liver cells, which aren't susceptible to HCV infection; in their place they transplanted human liver cells, which are. These mice with humanized livers could be infected with HCV[2]. "This was the first [mouse] model that actually allowed HCV infection for prolonged periods of time by the normal route," says Kneteman.

These animals have proven useful for testing many candidate drugs. For example, a Japanese team led by Hiroshima University's Kazuaki Chayama treated Kneteman's liver transplant mice with a combination of new drugs: the protease inhibitor telaprevir (from Vertex Pharmaceuticals, based in Cambridge, Massachusetts) and the experimental polymerase inhibitor MK-0608 (from drug giant Merck, headquartered in Whitehouse Station, New Jersey). Late last year, the team reported that this combination eliminated the virus from the animals after a month of therapy and prevented the emergence of drug resistance, which often arises in mice and humans treated with either drug alone[3].

But to facilitate the human tissue transplant, the mice must be engineered to lack components of their immune system. The animals are thereby rendered poor models for testing drugs that alter the immune system, known as immunotherapies. Generating these mice also presents special difficulties. For one,

researchers can't breed chimaeric animals. And the mice are sickly because of the liver toxic gene.

Two recent transplant models of HCV infection provide improvements over Kneteman's mice[4,5]. Both types of mouse are less frail because of technical workarounds that allow researchers to introduce the liver deficit later in life. The model developed by Lishan Su, an immunologist at the University of North Carolina at Chapel Hill, in collaboration with Ploss and Rice at Rockefeller, also involves transplanting human blood stem cells into the animals to reconstitute a human-like immune system[5]. Of all of the published reports, says Su, "this is the only one that has both the immune system and the human liver in a chimaeric animal", creating a living platform for testing vaccines and immunotherapies in a human-like model.

Even though Su's mice generate a human T-cell response against the virus when infected, they still lack a complete immune system. "What we need now is a mouse — an immunocompetent, normal, mouse — that can be infected by a hepatitis C virus capable of replicating, spreading and initiating an immune response," says Frank Chisari, a virologist at The Scripps Research Institute in La Jolla, California. "We are light years away from that because that virus does not like to infect or replicate in mouse cells." But scientists are getting closer.

ENTRY LEVEL POSITION

To gain entry into liver cells, HCV hijacks four proteins. Although mice naturally produce these proteins, the human versions of two of them are needed for viral entry[6]. The black rodents at Rockefeller are the first animals into which the required human entry factors have successfully been introduced. "This has a lot of applications," says Ploss. "Right now, it's useful to measure HCV entry and potential entry inhibitors."

"This is a big advance," says Michael Houghton, a virologist at the University of Alberta, who co-discovered HCV more than 20 years ago. "It's been difficult to do vaccine research for hepatitis C because of the lack of an animal model other than the chimp. Now we can start using different vaccine strategies in mice to see which are best at eliciting a protective response."

Ploss's mice are the first such animals with a fully intact immune system that are susceptible to the viral infection. But the infection stops after cell entry: the virus does not seem to replicate. "You can recapitulate HCV entry," says Ploss, "but replication is still very inefficient and not detectable by conventional methods." So the big challenge now remains identifying whether additional human factors are needed to achieve the next step of the HCV life cycle in mice.

After replication comes assembly, when the viral components are gathered into new infectious particles that will be released from the cell and invade other cells. Fortunately, this final stage in the viral life cycle seems to be possible in mouse cells without introducing any human proteins, according to research presented at this year's International Liver Congress, in Berlin, by Ralf Bartenschlager, a molecular virologist at Heidelberg University in Germany. If the barriers to replication can be overcome, Bartenschlager says, it should be straightforward to get a full infection cycle going in a mouse. "We have the early steps; we have the late steps; the big black box now is the step in between."

It took more than a decade for scientists to deduce the factors needed for HCV cell entry. But Thomas Baumert, a hepatologist and virologist at the University of Strasbourg in France, is confident that the community will solve the problem of replication much faster. "We have better model systems now, so I think we can advance more rapidly." Within five years, he predicts, "it will be possible to produce transgenic mice for the entire viral life cycle".

Rice is equally confident this approach will work — but he is hedging his bets. Even such a model would have its drawbacks, he says, because the more mouse-like the model, the further removed it is from the human system. That's why even as his lab is aggressively pursuing a transgenic animal, he maintains active collaborations to develop other models, including new transplant chimaeric mice with humanized livers and immune systems. Other researchers are looking to animals that provide the natural susceptibility of primates without the ethical baggage (see 'The turn of the shrew'). "All of these things should be pursued in parallel," Rice says, "because we really don't know which of these models is going to be the best for a given application."

And so Rice and others continue to try and build a better mouse to help the research community beat a path to new HCV treatments. ■

THE TURN OF THE SHREW

Unusual model isn't persuading researchers of its practicality

Although most of the work developing small-animal models of hepatitis C virus (HCV) infection has focused on mice, some research teams have advanced an alternative model: the northern treeshrew (Tupaia belangeri). This squirrel-shaped animal shares a common ancestor with apes and is the only non-ape species known to be naturally susceptible to HCV. Last year, the first longitudinal analysis of HCV-infected tree shrews showed that, over the course of three years, the animals developed chronic hepatitis, fatty liver degeneration and liver cirrhosis[7]. "It's very similar to HCV infection in human beings," says study co-author Kyoko Tsukiyama-Kohara of Kumamoto University in Japan.

But few research teams have managed to establish long-term infections in the animals. And given the limited track record of tree shrews in drug discovery, most scientists agree that more traditional lab animal models of infection, such as mice, are needed. "If you're going to take a multimillion dollar drug and do your final trial before you go into humans, you need to have a reproducible model," says Robert Lanford, who has studied HCV in chimps for more than 20 years at the Texas Biomedical Research Institute in San Antonio.

NEIL BOWMAN/FLPA

The northern treeshrew, a natural host to hepatitis C virus, is proving an unpopular model of infection.

Elie Dolgin *is a news editor with* Nature Medicine *in New York.*

1. Brenndörfer, E. D. *et al. Hepatology* **52**, 1553–1563 (2010).
2. Mercer, D. F. *et al. Nature Med.* **7**, 927–933 (2001).
3. Ohara, E. *et al. J. Hepatol.* **54**, 872–878 (2011).
4. Bissig, K. D. *et al. J. Clin. Invest.* **120**, 924–930 (2010).
5. Washburn, M. L. *et al. Gastroenterology* **140**, 1334–1344 (2011).
6. Ploss, A. *et al. Nature* **457**, 882–886 (2009).
7. Amako, Y. *et al. J. Virol.* **84**, 303–311 (2010).

Toxicology and Applied Pharmacology 260 (2012) 17–26

Contents lists available at SciVerse ScienceDirect

Toxicology and Applied Pharmacology

journal homepage: www.elsevier.com/locate/ytaap

Development of monoclonal antibodies to human microsomal epoxide hydrolase and analysis of "preneoplastic antigen"-like molecules

Hongying Duan [a,1], Kazunori Yoshimura [b,2], Nobuharu Kobayashi [a], Kazuo Sugiyama [a,3], Jun-ichi Sawada [c,4], Yoshiro Saito [c], Christophe Morisseau [d], Bruce D. Hammock [d], Toshitaka Akatsuka [a,*]

[a] Department of Microbiology, Faculty of Medicine, Saitama Medical University, Moroyama-cho, Iruma-gun, Saitama 350-0495, Japan
[b] Department of Physiology, Faculty of Medicine, Saitama Medical University, Moroyama-cho, Iruma-gun, Saitama 350-0495, Japan
[c] Division of Biochemistry and Immunochemistry, National Institute of Health Sciences, Kamiyoga 1-18-1, Setagaya-ku, Tokyo 158-8501, Japan
[d] Department of Entomology and Cancer Center, University of California, Davis, One Shields Avenue, Davis, CA 95616-8584, USA

ARTICLE INFO

Article history:
Received 17 September 2011
Revised 20 January 2012
Accepted 22 January 2012
Available online 28 January 2012

Keywords:
Microsomal epoxide hydrolase
Drug-metabolism
Monoclonal antibodies
Immunoassay
Tumor-associated antigens

ABSTRACT

Microsomal epoxide hydrolase (mEH) is a drug metabolizing enzyme which resides on the endoplasmic reticulum (ER) membrane and catalyzes the hydration of reactive epoxide intermediates that are formed by cytochrome P450s. mEH is also thought to have a role in bile acid transport on the plasma membrane of hepatocytes. It is speculated that efficient execution of such multiple functions is secured by its orientation and association with cytochrome P450 enzymes on the ER membrane and formation of a multiple transport system on the plasma membrane. In certain disease status, mEH loses its association with the membrane and can be detected as distinct antigens in the cytosol of preneoplastic foci of liver (preneoplastic antigen), in the serum in association with hepatitis C virus infection (AN antigen), or in some brain tumors. To analyze the antigenic structures of mEH in physiological and pathological conditions, we developed monoclonal antibodies against different portions of mEH. Five different kinds of antibodies were obtained: three, anti-N-terminal portions; one anti-C-terminal; and one, anti-conformational epitope. By combining these antibodies, we developed antigen detection methods which are specific to either the membrane-bound form or the linearized form of mEH. These methods detected mEH in the culture medium released from a hepatocellular carcinoma cell line and a glioblastoma cell line, which was found to be a multimolecular complex with a unique antigenic structure different from that of the membrane-bound form of mEH. These antibodies and antigen detection methods may be useful to study pathological changes of mEH in various human diseases.

Introduction

The microsomal epoxide hydrolase (mEH) is a drug-metabolizing enzyme that converts epoxides to diols and plays an important role in the metabolism of some mutagenic and carcinogenic epoxides (Newman et al., 2005). It is mainly expressed on the ER membrane in the liver (Newman et al., 2005) and constitutes about 2% of microsomal proteins (Gill et al., 1982). It was reported that mEH associates with various cytochrome *P450s* (Holder et al., 1974; Ishii et al., 2005), and functional cooperation between those enzymes is suggested (Taura et al., 2002). It is also expressed on the surface of hepatocytes (Zhu et al., 1999) and may act as a sodium-dependent bile acid transporter (von Dippe et al., 2003). In humans, mEH is the product of single locus (EPHX1) on chromosome 1. Several single nucleotide polymorphism sequences were found in association with the onset of several diseases and cancers (McGlynn et al., 1995; Park et al., 2005; Smith and Harrison, 1997; Sonzogni et al., 2002). Association of the mEH with cancers and diseases has been further suggested by the following observations. The mEH was identified as the brain tumor antigen in some glioblastoma cell lines (Kessler et al., 2000). Although mEH is

Abbreviations: mEH, microsomal epoxide hydrolase; ER, endoplasmic reticulum; ELISA, enzyme-linked immunosorbent assay; PAGE, polyacrylamide gel electrophoresis; CsCl, cesium chloride; PCR, polymerase chain reaction; IPTG, isopropyl β-D-thiogalactoside; GST, glutathione S-transferase; TMB, 3, 37, 5, 57-tetramethylbenzidone; BCIP, 5-bromo-4-chloro-3-indoyl-phosphate; NBT, nitroblue tetrazolium; PBS, phosphate-buffered saline; BSA, bovine serum albumin; HRP, horseradish peroxidase; FCS, fetal calf serum; CBA, competitive antibody binding assay; S-mEH, solubilized form of mEH; M-mEH, membrane-bound form of mEH; L-mEH, linearized form of mEH; RIA, radioimmunoassay; PNA, preneoplastic antigen; HCC, hepatocellular carcinoma; HCV, hepatitis C virus; OD, optical density.

* Corresponding author. Fax: +81 49 295 9107.
E-mail address: akatsuka@saitama-med.ac.jp (T. Akatsuka).
[1] Present address: Laboratory of Hepatitis Viruses, Division of Viral Products, Center for Biologics Evaluation, Food and Drug Administration, Bethesda, MD 20892, USA.
[2] Present address: Department of Rehabilitation, Nihon Institute of Medical Science, 1276 Simokawahara, Moroyama-cho, Saitama 350-0435, Japan.
[3] Present address: Center for Integrated Medical Research, Keio University, Shinanomachi 35, Shinjuku-ku, Tokyo 160-8582, Japan.
[4] Present address: Pharmaceuticals and Medical Devices Agency, 3-3-2 Kasumigaseki, Chiyoda-ku, Tokyo 100-0013, Japan.

0041-008X/$ – see front matter © 2012 Elsevier Inc. All rights reserved.
doi:10.1016/j.taap.2012.01.023

tightly associated with membranes in normal cells, the mEH is sometimes detected in the cytosol of neoplastic human livers and released into the blood (Gill et al., 1983). The appearance of mEH in the blood is also associated with other types of liver disease (Hammock et al., 1984). In hepatitis C infection, we have shown that the hepatitis C-associated antigen (AN antigen) appears in the early phase of the viral infection (Akatsuka et al., 1986b), which is followed by the development of the antibody in the acute phase of hepatitis (Akatsuka et al., 1986a). In a recent study, we have shown that the AN antigen is mainly composed of mEH (Akatsuka et al., 2007). These lines of evidence suggest that mEH loses the association with membranes in some disease processes which are accompanied by the changes of its structure. To enable us to analyze the changes of mEH status in situ, we developed monoclonal antibodies against different parts of mEH molecule and antigen detection methods which can quantitate differentially the membrane-bound form and soluble form of mEH.

Materials and methods

Cell lines. Sf9 was a gift from Dr. Stephen M. Feinstone (CBER, FDA) and cultured in Sf900II SFM (Invitrogen, Carlsbad, CA) at 27 °C. The hepatocellular carcinoma (HCC) cell lines, Huh-1 (Huh et al., 1982) and Huh-7 (Nakabayashi et al., 1982) were obtained from the Japanese Cancer Research Resources Bank. Huh-1 was cultured in RPMI1640 with 10% FCS; Huh-7 was cultured in RPMI1640 with 2% FCS and 30 nmol/l $Na_2 2SeO_3$. THLE-5b, a normal liver cell line which was immortalized by transfecting with the plasmid containing SV40 T antigen (Lechner et al., 1991), was a gift from Dr. Curt C. Harris (NCI, NIH) and cultured in RPMI1640 with 5% FCS. Human fibroblast cell line M1 (Royer-Pokora et al., 1984) was a gift from Dr. William E. Biddison (NIAID, NIH). Glioblastoma cell lines U87MG (Ishii et al., 1999) and LN-Z308 (Albertoni et al., 1998) were gifts from Dr. Ryo Nishikawa (Saitama Medical Univ., Japan) and LN-71 (Ishii et al., 1999) was a gift from Dr. Erwin G. Van Meir (Emory Univ.). These four cell lines were cultured in DMEM with 10% FCS. Myeloma cell line NS-1 was a gift from Dr. Mineo Arita (National Institute of Infectious Diseases, Japan) and cultured in RPMI1640 with 15% FCS.

Purified mEH antigens. Expression of human mEH in a recombinant baculovirus system (Morisseau et al., 2001) and the purification procedure of the solubilized form of mEH (Akatsuka et al., 2007) have been described. Briefly, the infected cells were solubilized with Triton X-100 and subjected to Q-Sepharose column chromatography. Antigen-positive fractions were pooled and stored in a buffer containing 0.05% Triton X-100. A part of this preparation (the solubilized form of mEH, S-mEH) was used for ELISA screening of hybridoma cultures, and the rest was submitted for preparative SDS-PAGE to obtain the linearized form of mEH (L-mEH) which was used for immunization of mice, competitive antibody binding assays, and as the standard for antigen detection assays. The preparative SDS-PAGE was performed by applying 1.0 mg of the S-mEH to Model 491 PrepCell (Bio-Rad, Hercules, CA) consisting of a 40 ml polyacrylamide (10%) gel and a 6 ml stacking gel. During electrophoresis at 12 W, proteins were eluted with running buffer with a flow rate of 0.5 ml/min, and 3.5 ml fractions were collected. Each fraction was tested by dot blot assay on an Immobilon-P membrane (Millipore, Bedford, MA) using rabbit anti-mEH antibody (Akatsuka et al., 2007), and then, aliquots of antigen-positive fractions were subjected to a 10% minigel (Mini-Protean; Bio-Rad, Hercules, CA) for silver staining. Factions with a homogenous 47 kDa band were pooled, applied to a 0.4 ml Extracti-Gel column (Pierce, Rockford, IL), and after elution with PBS containing 0.05% Triton X-100, concentrated with Centriplus YM-10 (Millipore, Bedford, MA). Purification of the membrane-bound form of mEH (M-mEH) has been described (Akatsuka et al., 2007). Briefly, a homogenate of recombinant baculovirus-infected Sf9 cells was first passed through a gel-filtration column (Sephacryl S-300, Amersham, Uppsala, Sweden). The void volume fraction was then subjected to ultracentrifugation in a sucrose-gradient followed by a second ultracentrifugation in a CsCl gradient. Each fraction was tested by an antibody sandwich ELISA using horseradish peroxidase (HRP)-labeled anti-AN antigen monoclonal antibody 1F12, and positive fractions were pooled and concentrated with Centriplus YM-100 (Millipore, Bedford, MA). Protein concentration was measured by micro BCA assay (Pierce, Rockford, IL).

GST-mEHs. A full-length and eight truncated human mEH cDNAs (Fig. 1) were amplified using the mEH cDNA (Akatsuka et al., 2007) by PCR with KOD-Plus polymerase (Toyobo, Tokyo, Japan) and primers shown in Table 1. The PCR products were digested with *Bam*HI and *Sma*I, and ligated into the same cloning sites of pGEX-2T (GE Healthcare, Uppsala, Sweden). Competent BL21 cells of *E. coli* were transformed with the recombinants, and after IPTG induction (0.1 mM, 5 h), 1 ml culture of the cells was extracted with 300 μl of SDS sample buffer and used as the ELISA antigen.

SDS-PAGE and Western blotting. For Coomassie blue staining and immunoblotting of GST-mEH produced by *E. coli*, 13 and 5 μl of cell suspensions were extracted with SDS sample buffer and applied onto a 10% minigel (Mini-Protean; Bio-Rad), respectively. After separation and transfer to an Immobilon-P membrane (Millipore, Bedford, MA), the antigen was detected with goat anti-GST (Amersham, Buckinghamshire, UK) (1:1000) followed by HRP-labeled rabbit anti-goat IgG (KPL, Gaithersburg, MA) and TMB substrate (KPL), or with mouse anti-mEH obtained in this study (1:500) followed by alkaline phosphatase-labeled goat anti-mouse IgG (KPL) and BCIP/NBT substrate (KPL), respectively. For the immunoblotting of mEH-expressing cell lines, 1×10^5 cells were extracted in 25 μl of SDS sample buffer and applied onto a 10% minigel. The transferred antigen was detected with the culture supernatant of anti-mEH hybridoma culture (1:10) followed by alkaline phosphatase-labeled goat anti-mouse IgG (KPL) and BCIP/NBT substrate (KPL).

ELISA for antibody detection. Each well of 96-well ELISA plates (Costar, Acton, MA) received 50 μl of one of the following antigen solutions diluted in PBS: M-mEH, S-mEH, and L-mEH, 0.4 μg/ml; GST-mEH, (1:250) dilution; and the mEH peptide aa 54–71, 0.5 μg/ml. After incubation at 4 °C overnight, the well was washed with PBS containing 0.05% Tween 20 (PBS-T) and blocked with 200 μl of PBS containing 5% BSA (blocking solution) for 1 h at 37 °C. After washing, 50 μl of culture supernatants, ascitic fluids, or sera diluted in PBS containing 1% BSA (dilution buffer) was added and incubated at 37 °C for 1 h. Each well was washed three times and received 50 μl of HRP-conjugated anti-mouse IgG or anti-rabbit IgG (H- and L-chain specific) (KPL, Gaithersburg, MA) which was diluted 1:1000 (0.5 μg/ml) with PBS containing 10% FCS. After incubation at 37 °C for 1 h and washing, the color was developed by adding 200 μl of *o*-phenylenediamine dihydrochloride substrate (SIGMA, St. Louis, MO), and the reaction was stopped by adding 50 μl of 6 N H_2SO_4. The plates were measured at an optical density of 492 nm. We previously described the aa 54–71 mEH peptide, the rabbit antibody against this peptide (Maekawa et al., 2003), and the rabbit anti-mEH antibody (Akatsuka, et al., 2007).

Monoclonal antibodies. Two female BALB/c mice (age, 6 weeks) were purchased from Tokyo Laboratory Animal Science Co. Ltd. (Tokyo, Japan). They were injected s.c. with 2 μg of L-mEH four times (first with Freund's complete adjuvant, second with incomplete adjuvant, third and fourth immunizations without adjuvant) at one- to two-month intervals. Two months thereafter, they were boosted i.p. with 40 μg of L-mEH, and after another 3 days, their spleen cells were harvested. Hybridization of spleen cells with myeloma cells NS-1 was performed as described (Akatsuka et al., 1986b), and culture supernatants were tested for anti-mEH activity by ELISA using S-mEH as the antigen. Antibody-secreting cells were cloned three times or more by

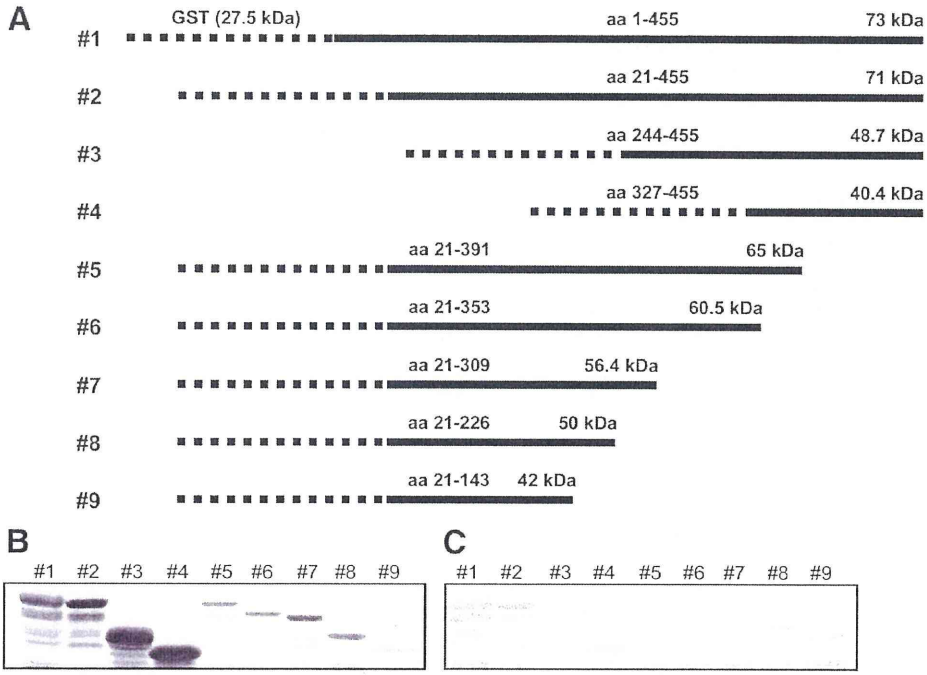

Fig. 1. Full-length and truncated mEH expressed as GST fusion proteins in *E. coli*. A, schematic representation of nine kinds of GST-mEH (F-mEH) used for epitope mapping. A predicted size (shown by kDa) of a GST-mEH from each construct is shown on the right. Expressed antigens were detected by Western blotting with goat anti-GST (B) and mouse anti-mEH (C) polyclonal antibodies and confirmed to have the expected molecular sizes.

limiting dilution with the culture medium containing 10% BM-Conditioned H1 (Roche, Mannheim, Germany). Ascitic fluids were obtained by injecting hybridomas i.p. into pristane (SIGMA)-primed BALB/c nude mice (Clea Japan, Tokyo, Japan) ($1–5\times10^6$ cells/mouse). Antibody isotype was determined with mouse monoclonal antibody isotyping kit (GE Healthcare) following the manufacturer's instructions.

Competitive antibody binding assay. Competitive antibody binding assay (CBA) was performed following the procedure described elsewhere (Stone and Nowinski, 1980). A flat-bottomed eight well strip plate (Costar) was used as the solid phase and 50 μl of L-mEH diluted (0.4 μg/ml) in PBS was added to each well and incubated overnight at 4 °C. For the assays between the type V and the anti-AN antibody, M-mEH was coated instead of L-mEH to each well. After blocking with 200 μl of blocking solution for 1 h at 37 °C and washing, 50 μl of unlabeled IgG (5-fold dilutions in dilution buffer starting from 5 μg/ml) was incubated in each well at 37 °C for 1 h. Then, 2×10^5 cpm of ^{125}I-labeled IgG in 50 μl of dilution buffer was added and incubated at 37 °C for 1 h. Each well was separated after washing, and the bound radioactivity was counted by a gammacounter. IgG was purified from ascitic fluid using Protein G Sepharose (GE Healthcare) following the manufacturer's instructions, and labeling with ^{125}I was performed by the chloramine-T method (Mcconahey and Dixon, 1966).

ELISA and RIA for Ag detection. IgG was labeled with ^{125}I as described above or with HRP using Peroxidase Labeling Kit (Dojindo, Kumamoto, Japan). Antibody sandwich RIA and ELISA were performed using flat-bottomed eight well strip plates (Costar) and 96-well ELISA plates (Costar), respectively. Each well adsorbed 50 μl of unlabeled IgG (5 μg/ml in PBS; 1 h at 37 °C), and after washing with PBS-T and blocking, received 50 μl of antigen solution in dilution buffer. After incubation and washing, 1×10^5 cpm of ^{125}I-labeled IgG or HRP-labeled IgG in 50 μl of dilution buffer was added, and after another incubation and washing, the bound radioactivity was counted by a gammacounter or the color was developed by adding *o*-phenylenediamine dihydrochloride substrate as described above for CBA and Ag binding ELISA. Culture supernatants used for mEH antigen detection were prepared as follows: the cells were seeded in 10-cm dishes, and after 4 days incubation (~80% confluency), the supernatant was collected, and after centrifugation at 30,000×*g* for 10 min, filtrated through a 0.45 μM filter and stored at −80 °C until use. Aliquots of the culture supernatant were concentrated about 10-fold by ultrafiltration through

Table 1
Primers for the amplification and expression of mEH fragments.

Primer	Sequence[a]	Description
1	5′-CGGGATCCATGTGGCTAGAAATCCTCCTCAC-3′	Sense primer for #1
2	5′-CGGGATCCCGGGACAAAGAGGAAACTTTGCC-3′	Sense primer for #2, #5–#9
3	5′-CGGGATCCAAAGGCCTGCACTTGAACATGGC-3′	Sense primer for #3
4	5′-CGGGATCCGAGAAGTTTTCCACCTGGACC-3′	Sense primer for #4
5	5′-CGGGATCCTTGCCGCTCCAGCACCGACAGG-3′	Antisense primer for #1
6	5′-TCCCCCGGGTTGCCGCTCCAGCACCGACAGG-3′	Antisense primer for #2–#4
7	5′-TCCCCCGGGCTTCATCCGCTCACGCTTCTG-3′	Antisense primer for #5
8	5′-TCCCCCGGGGTCGTCCAGGGAGAACTTCC-3′	Antisense primer for #6
9	5′-TCCCCCGGGGGTGTCAGGCTTGGTGCACTG-3′	Antisense primer for #7
10	5′-TCCCCCGGGGTCCCCTCCTTGAATGTAGAA-3′	Antisense primer for #8
11	5′-TCCCCCGGGGGGCTTCGGGGTATGGCCTGC-3′	Antisense primer for #9

[a] The underlined sequences GGATCC and CCCGGG represent recognition sequences of *Bam*HI and *Sma*I, respectively.

Table 2
Epitope mapping of anti-mEH monoclonal antibodies by ELISA. Mean OD values of duplicate ELISA are indicated, and positive results are highlighted in gray. The cut-off was determined as the mean ± 5 standard deviations of NS-1 culture supernatants (0.113) and that of the naïve mouse sera (0.202), for hybridoma cultures and the immune mouse sera, respectively.

	F-mEH									
Antibody	1	2	3	4	5	6	7	8	9	pGEX
2D8	2.790	2.637	0.059	0.067	2.721	2.833	2.695	2.686	2.757	0.055
5D8	2.551	2.365	0.092	0.063	1.824	1.972	2.055	2.051	2.001	0.053
8F11	2.519	2.330	0.090	0.050	1.819	1.663	2.065	2.043	1.852	0.053
K4F8	2.473	2.354	0.105	0.096	1.785	1.931	1.987	1.938	1.752	0.062
K2B7	2.527	2.395	0.086	0.082	0.913	0.930	1.341	1.475	0.637	0.059
6E3	2.120	2.029	2.779	2.770	0.214	2.022	0.064	0.068	0.075	0.032
2G2	0.000	0.000	0.000	0.000	0.000	0.000	0.000	0.000	0.000	0.000
7B11	0.007	-0.016	-0.027	0.031	-0.026	-0.101	-0.023	-0.048	-0.041	0.001
NS-1	0.061	0.070	0.046	0.077	0.062	0.064	0.057	0.052	0.045	0.045
Immune	1.657	1.417	2.199	2.092	1.199	1.204	1.424	1.288	1.185	0.117
Naïve	0.060	0.046	-0.015	0.048	0.064	-0.009	0.058	0.051	0.087	0.038

a 10 kDa cut-off membrane (Centriplus YM-10, Millipore) and half of each concentrate was further subjected to ultrafiltration through a100 kDa cut-off membrane (Centricon YM-100, Millipore) and the flow-through fractions were collected.

Analysis of mEH activity in culture media and inhibitory activity of monoclonal antibodies. Concentrated culture media were dissolved 10 fold in Tris/HCl buffer (0.1 M pH 9.0) containing 0.1 mg/ml BSA and the activities were measured with [^{3}H]-*cis*-stilbene oxide after incubation for 15 min at 30 °C (Morisseau et al., 2001). Purified human mEH (S-mEH) diluted 100-fold was used as positive control, and protein content was measured with BCA assay (Pierce, Rockford, IL) using BSA as standard. Detection limit in this condition was around 0.3 nmol min^{-1} ml^{-1}. Monoclonal antibodies were diluted 10^7 fold in the same buffer as above and incubated with S-mEH. mEH inhibitor, 2-nonylthio-propiamide (NTPA) was used at 100 μM as the positive control.

Results

Preparation of mEH antigens for immunization and antibody detection

We developed monoclonal antibodies which recognize different portions of human mEH. The solubilized form of mEH (S-mEH) was purified as described previously (Akatsuka et al., 2007) and used for the screening of hybridomas. A part of S-mEH was submitted for preparative SDS-PAGE to obtain the linearized form of mEH (L-mEH) and used for immunization of mice, because we wished to obtain antibodies against the linear epitopes of mEH (see Discussion). For epitope mapping of monoclonal antibodies, we expressed nine mEH fragments (F-mEH) with truncations at the N-terminus or the C-terminus as GST-fusion proteins in *E. coli* (Fig. 1A). SDS-PAGE followed by Coomassie Blue staining (data not shown) or immunoblotting with an anti-GST antibody (Fig. 1B) and anti-mEH antibody (Fig. 1C) revealed that each mEH fragment with the predicted size was successfully expressed in *E. coli*. ELISA testing using the F-mEH 1 to 4 as the antigens showed that the immunized mice developed antibodies against F-mEH 1 and 2 but not 3 or 4 after the first and the second immunizations. Antibodies which reacted with all the four antigens appeared only after the third immunization, which suggested that the N-terminus of mEH had higher immunogenicity than the C-terminus (data not shown).

Development of monoclonal antibodies against mEH

After we confirmed that the two immunized mice developed antibodies to F-mEH 1 to 4, we established hybridomas. In two separate fusions, sixty-five colonies were found to produce antibodies against the S-mEH, among which 23 antibodies reacted only with F-mEH 1 and 2, 16 reacted with F-mEH 1 to 4, and 26 reacted only with the S-mEH. Eight hybridomas were subjected to limiting dilution three times or more, and tested by ELISA using all of the GST-mEH antigens (F-mEH 1 to 9). The results shown in Table 2 suggest that the five antibodies (2D8, 5D8, 8F11, K4F8, and K2B7) recognize the N-terminus (aa 21–143, F-mEH 9), and 6E3 recognizes the C-terminus (aa 327–353, F-mEH 4). Antibodies 2G2 and 7B11 reacted with the S-mEH but not with any of the F-mEH 1 to 9, therefore, they seemed to recognize the conformational epitope which was lost during the preparation of the F-mEHs by SDS treatment (Fig. 2). This speculation was substantiated by the ELISA in which the antibodies were tested against the three antigens: the S-mEH, the L-mEH, and the membrane-bound form of mEH (M-mEH). The antibodies 2G2, 7B11, and the anti-AN antigen monoclonal antibodies 1H9 and 1F12, which recognize the three-dimensional structure of mEH (Akatsuka et al., 2007), reacted with M-mEH and S-mEH but not with L-mEH.

The six antibodies which reacted with one or more of the F-mEH 1 to 9 seemed to recognize linear structures of mEH, and were tested for their reactivity in Western blotting using three kinds of mEH-expressing cell lines: Sf9 cells infected with a recombinant baculovirus (Fig. 3A), THLE-5b, a normal human liver cell line which was immortalized by transfecting with the plasmid containing SV40 T-antigen (Lechner et al., 1991) (data not shown), and a hepatocellular carcinoma

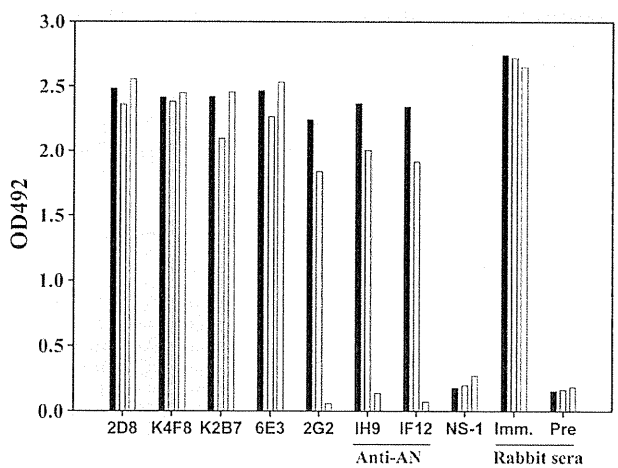

Fig. 2. ELISA test for the measurement of antibody reactivity to M-mEH (black bars), S-mEH (gray bars), and L-mEH (white bars). Ascitic fluids of hybridomas (1:1000 dilution) and the rabbit anti-mEH antiserum (1:200 dilution) were tested. The ascitic fluid of NS-1 cells and the preimmune rabbit serum were used as the negative controls.

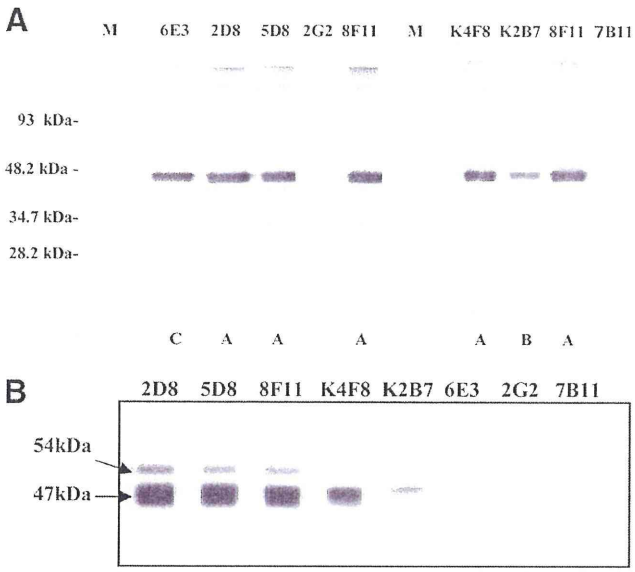

Fig. 3. Reactivity of anti-mEH monoclonal antibodies against the immunoblots of mEH-expressing cell lines. 10% SDS gel was loaded with molecular weight marker (M), mEH-expressing Sf9 cell extract (A), and Huh-1 cell extract (B), and underwent Western blotting. The immunoblot was detected with anti-mEH antibodies followed by alkaline phosphatase-labeled second antibody. The patterns (A–C) of the bands on the blot of Sf9 cell extract (A) are shown at the bottom of the figure.

(HCC) cell line, Huh-1 (Huh et al., 1982) (Fig. 3B). When extracts of each of the three cell lines were blotted, all of the six antibodies showed 47 kDa bands, the size of which corresponded to the whole mEH molecule. In the blotting of mEH-expressing Sf9 cells (Fig. 3A), additional smaller bands, which may be degradation products of mEH, could be seen, and the pattern of the bands could be divided into three types: type A for 2D8, 5D8, 8F11 and K4F8; type B for K2B7; and type C for 6E3. Based on these patterns of bands, the five antibodies which recognize the N-terminus (aa 21–143) could be separated into the two groups: type A group (2D8, 5D8, 8F11 and K4F8) and type B group (K2B7) (Table 3). In the blotting of the hepatocyte-derived cell lines THLE-5b and Huh-1, a higher band of 54 kDa could be seen with the three out of four antibodies in the type A group (2D8, 5D8 and 8F11), but not with K4F8 in the same type A group or other four antibodies (Fig. 3B). Therefore, the four antibodies in the type A group could be further divided into the two groups: 2D8, 5D8 and 8F11 (type A1), which cross-react with a molecule of 54 kDa protein, and K4F8 (type A2), which only recognizes a 47 kDa band (Table 3). Therefore, the eight antibodies could be divided into the five types (type I to V) depending on their epitope specificities (Table 3).

The epitope specificity of the antibodies was further tested by competitive antibody binding assay (CBA) in which a constant amount of ^{125}I-labeled antibody was allowed to compete with increasing concentrations of the unlabeled homologous or heterologous antibodies for binding to L-mEH. As an unlabeled antibody, rabbit antiserum which was raised against a peptide (aa 54–71) (Maekawa et al., 2003) was also included. As shown in Table 4, binding of labeled 5D8 was inhibited by 2D8 as well as by homologous unlabeled 5D8, but not by other types of antibodies, which indicates the two kinds of type I antibodies (2D8 and 5D8) recognize the same or closely adjacent epitopes. Binding of K4F8 (type II) was greatly inhibited by the two type I antibodies as well as homologous K4F8. Although inhibition of binding of labeled 5D8 by unlabeled K4F8 was relatively low, type I and type II antibodies seemed to recognize distinct but adjacent epitopes on mEH. Binding of labeled K2B7 was almost completely inhibited by the rabbit anti-peptide antibody as well as by homologous unlabeled K2B7, which indicated that the epitope of type III overlaps with the region of aa 54–71. Binding of labeled 6E3 was inhibited only by homologous unlabeled 6E3. CBA was also performed for the antibodies which recognize conformational epitopes using M-mEH as the antigen. Binding of type V antibody 2G2 was found to be inhibited not only by homologous 2G2 but also by 1H9 which had been developed against the AN antigen purified from the liver of a patient with hepatitis C (Akatsuka et al., 1986b) and later proved to be highly selective for a conformational epitope on the membrane-bound form of mEH (Akatsuka et al., 2007). To confirm the possibility that the epitope of K2B7 (type III) overlaps with aa 54–71, we tested the antibodies by ELISA with the peptide aa 54–71 coated to the plates, and found that only K2B7 and the rabbit antiserum revealed significant reactivity with the peptide (Fig. 4). Taken together, the epitope selectivity of the five types of the antibody can be summarized as shown in Table 5. These five types of antibodies were tested if they inhibit mEH catalytic activity, but any of the antibodies did not reveal significant inhibition against purified recombinant human mEH (S-mEH) (less than 13.3%, data not shown).

Development of mEH antigen detection systems

Previously, we have detected a hepatitis C-related antigen (AN-antigen) in sera from patients with hepatitis C (Akatsuka et al., 1986b) and chimpanzees experimentally infected with hepatitis C virus (HCV) (Akatsuka et al., 1986a) by radioimmunoassay (RIA) using anti-AN-antigen monoclonal antibody, 1F12. Recently, we have shown that most of the antigenicity of AN-antigen consists of mEH and anti-AN-antigen monoclonal antibodies recognize conformational epitopes of mEH (Akatsuka et al., 2007). The antigen was somewhat similar to preneoplastic antigen (PNA) which had been described as an antigen in preneoplastic foci in livers that is released into the blood (Okita and Farber, 1975), and later found to be immunologically identical to mEH (Levin et al., 1978). The mEH has been also reported to reveal a somewhat anomalous antigenicity in some glioblastoma cell lines (Kessler et al., 2000). To assess the similarity between PNA, AN-

Table 3
Classification of anti-mEH monoclonal antibodies. Eight monoclonal antibodies were grouped into five groups (Type I to V) depending on the reactivity with F-mEH 1 to 4 and S-mEH by ELISA, and the band sizes and patterns they produced in Western blotting. Their H-chain and L-chain isotypes are also shown.

Clone	Isotype	L-chain	ELISA					Western blotting			
			F-mEH								
			1	2	3	4	S-mEH	Sf9	THLE-5b	Huh-1	Type
2D8	G2a	κ	+	+	−	−	+	A1	54 K, 47 K	54 K, 47 K	I
5D8	G1	κ	+	+	−	−	+	A1	54 K, 47 K	54 K, 47 K	I
8F11	G1	κ	+	+	−	−	+	A1	54 K, 47 K	54 K, 47 K	I
K4F8	G1	κ	+	+	−	−	+	A2	47 K	47 K	II
K2B7	G1	κ	+	+	−	−	+	B	47 K	47 K	III
6E3	G1	κ	+	+	+	+	+	C	47 K	47 K	IV
2G2	G1	κ	−	−	−	−	+	−	−	−	V
7B11	M	κ	−	−	−	−	+	−	−	−	V

Table 4
Competitive binding assay. Six kinds of antibodies were labeled with ^{125}I, and 2×10^5 cpm of each antibody was incubated with increasing concentrations of the unlabeled homologous or heterologous antibodies in the wells coated with mEH. As the antigen, L-mEH was used for the antibodies from type I to type IV and the rabbit anti-peptide aa54–71 antibody. M-mEH was used for the type V and anti-AN antibodies. % inhibition values at 5 μg/ml are shown, and those above 80% are highlighted in gray.

^{125}I-antibody		Unlabeled antibody						
		Type I		Type II	Type III	Type IV	Type V	Anti-AN	Rabbit Ab
Type	Clone	2D8	5D8	K4F8	K2B7	6E3	2G2	1H9	aa54-71
Type I	5D8	96.1	100.0	62.6	30.9	38.0	1.4	1.4	4.2
Type II	K4F8	93.9	94.7	100.0	16.9	10.5	15.5	15.5	25.9
Type III	K2B7	28.4	54.2	72.0	100.0	39.7	0.0	0.0	99.3
Type IV	6E3	30.0	26.2	43.4	44.0	100.0	43.0	43.0	51.6
Type V	2G2	N.D.	17.9	N.D.	N.D.	9.1	100.0	100.0	N.D.
Anti-AN	1H9	N.D.	14.1	N.D.	N.D.	10.7	87.8	100.0	N.D.

N.D.: not determined.

antigen, and the brain tumor antigen, and their differences from the normal mEH bound to the membrane, we developed sensitive mEH antigen detection assay systems using the monoclonal antibodies. Among the five types of antibodies, type I antibodies which cross-react with a 54 kDa protein were excluded, and K4F8 (type II), K2B7 (type III), 6E3 (type IV), and 2G2 (type V) were labeled with ^{125}I or horseradish peroxidase (HRP). Two kinds of the purified mEH obtained from recombinant baculovirus-infected Sf9 cells were used as the antigen standards. The membrane-bound form of mEH was purified by density gradient centrifugation without using detergents (Akatsuka et al., 2007) (M-mEH); the linearized form of mEH (L-mEH) was described above. We tried to detect the antigens by antibody sandwich RIA and ELISA methods using several combinations of unlabeled and labeled antibodies. As shown in Table 6 (titration curves of three kinds of ELISA are shown in Fig. 5), M-mEH was successfully detected by the combinations between type V and homologous or heterologous antibodies; the homologous combination (V–*V) was the most sensitive (Fig. 5A) followed by the combination of unlabeled type IV and labeled type V (IV–*V) (Fig. 5B). L-mEH could be detected by the combination of unlabeled type IV and labeled type II antibodies (IV–*II) (Fig. 5C). Interestingly, M-mEH could not be detected with satisfactory sensitivity by IV–*II (Fig. 5C) or by any other combinations of antibodies excluding type V (Table 6). Importantly, the sandwich assay method based on the combination of IV–*II enables us to detect the mEH antigen in multiple forms only if it is denatured with detergents such as SDS before incubation for the assay.

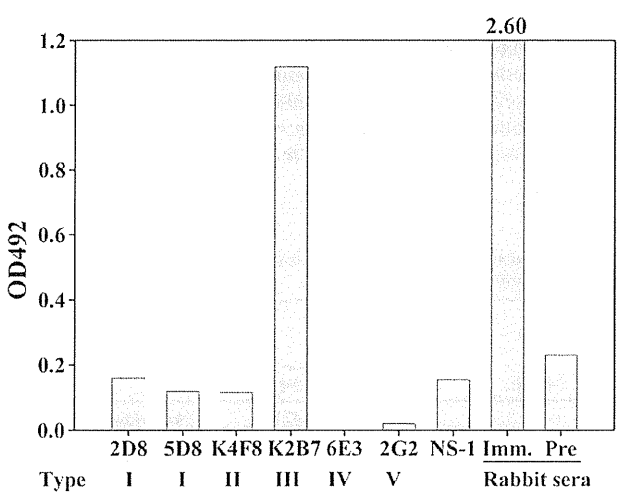

Fig. 4. Reactivities of anti-mEH monoclonal antibodies against the mEH peptide aa 54–71 were tested by ELISA. Ascitic fluids of hybridomas (1:1000 dilution) and the rabbit anti-peptide aa 54–71 antiserum (1:200 dilution) were tested. The ascitic fluid of NS-1 cells and the preimmune rabbit serum were used as the negative controls.

Analyses of antigenic structure of PNA-like mEH antigens

We applied three kinds of RIAs with the antibody combinations, IV–*II, IV–*V, and V–*V to the detection of mEH in culture supernatants of seven cell lines (Table 7). Two lines (THLE-5b and Huh-1) were also used for Western blotting in this study (Table 3). THLE-5b (Lechner et al., 1991) was derived from normal human hepatocytes which were immortalized by transfection of SV40 T antigen gene, and maintain many functions of normal hepatocytes including phase II drug-metabolizing enzymes. Huh-7 (Nakabayashi et al., 1982) is a well-differentiated HCC cell line and secretes a variety of major plasma proteins; e.g., albumin, transferrin alpha-fetoprotein and the acute phase proteins. Huh-1 (Huh et al., 1982) is a HBs antigen-producing undifferentiated HCC line and produces tumors in nude mice. M1 is a cell line derived from human fibroblasts (Royer-Pokora et al., 1984). LN-71 (Ishii et al., 1999), LN-Z308 (Albertoni et al., 1998), and U87MG (Ishii et al., 1999) are human glioblastoma cell lines; LN-71 was described as brain tumor antigen BF7/GF2 positive whereas LN-Z308 as negative (Kessler et al., 2000). All the cell lines were found to express mEH with a 47 kDa band which was detected by the type II antibody K4F8 in Western blotting (data not shown). Significant signals were obtained from the supernatants of Huh-1 and LN-71 by the V–*V method. Those antigens could not be detected by the IV–*V method even though the amounts exhibited by V–*V method (4.26 and 7.83 ng/ml) were higher than the detection limit of IV–*V (1.6 ng/ml). They could not be detected by the IV–*II method either. Since we did not add detergent before this assay, the mEH in these supernatant may have been folded in a shape which is undetectable by the IV–*II assay. We speculated that this folding is somehow different from that of M-mEH in that the type IV epitope is hindered inside the mEH molecule in the supernatant and undetectable by the IV–*V method.

For further analysis, we concentrated the supernatants of THLE-5b, Huh-1 and LN-71 cultures about 10-fold by ultrafiltration through 10 kDa cut-off membranes. Then aliquots of these concentrates as

Table 5
Epitope selectivities of five types of monoclonal antibodies.

Type I	N-terminus (aa.21–143) linear epitope, Cross-reacts with a 54-kDa protein
Type II:	N-terminus (aa.21–143) linear epitope
Type III:	N-terminus (aa.54–71) linear epitope
Type IV:	C-terminus (aa.327–353) linear epitope
Type V:	Conformational epitope

Table 6
mEH detection by antibody sandwich methods.

Five kinds of monoclonal antibodies were labeled with ^{125}I or horse radish peroxidase (denoted by the asterisk), and used for detection of the purified mEH antigens (membrane-bound form of mEH: M-mEH or linearized form of mEH: L-mEH) which had been captured by the unlabeled homologous or heterologous antibodies (without asterisk) coated on the wells of 96-well plates. Signal/noise (S/N) ratios at 40 ng/ml of the antigen concentration are shown, and those above 10.0 are highlighted in gray.

RIA			ELISA		
Ab combinations	Antigen	S/N ratio	Ab combinations	Antigen	S/N ratio
II–*IV	M-mEH	1.8	II–*V	M-mEH	36.6
	L-mEH	1.8		L-mEH	N.D.
III–*IV	M-mEH	1.4	III–*V	M-mEH	20.2
	L-mEH	1.8		L-mEH	N.D.
IV–*II	M-mEH	2.5	IV–*V	M-mEH	48.4
	L-mEH	15.4		L-mEH	N.D.
IV–*III	M-mEH	2.0	V–*V	M-mEH	52.7
	L-mEH	9.0		L-mEH	N.D.
V–*V	M-mEH	15.4	IV–*II	M-mEH	1.9
	L-mEH	<1.0		L-mEH	15.7

N.D.: not determined.

well as the standard antigens, M-mEH and L-mEH, were subjected to ultrafiltration through 100 kDa cut-off membranes, and the flow-through fractions were obtained. When we measured these samples by the three antigen detection ELISA methods, the media of THLE-5b did not show positive signals. On the other hand, the mEHs in the supernatants of Huh-1 and LN-71 were well detected by V–*V, and we found that the detected antigens did not pass through the 100 kDa cut-off membranes indicating that they were in the shape of a multimolecular complex larger than 100 kDa (Fig. 6A). However, in contrast to M-mEH, the mEHs in the supernatants of Huh-1 and LN-71 could scarcely be detected by IV–*V (Fig. 6B) as was observed for the unconcentrated supernatants (Table 7). When we tested these samples by IV–*II without adding SDS, only L-mEH could be detected (data not shown). After addition of SDS, the antigens in the supernatants of the two cell lines, M-mEH as well as L-mEH could be detected, and we found that part of the antigens in the supernatants and most of L-mEH passed through the 100 kDa cut-off membranes (Fig. 6C). We could also see positive signals from the supernatant of THLE-5b especially after ultrafiltration through the100 kDa cut-off membrane. In addition, all of the three culture media showed significant mEH activity (0.025–0.046 nmol min^{-1} mg^{-1}). These results suggested that all of the three cell lines secrete a small amount of mEH with the size smaller than 100 kDa probably existing as single molecules folded in particular shapes which could not be detected by either of the IV–*II (without detergent treatment), V–*V, or IV–*V method. The majority of the mEH in the supernatants of Huh-1 and LN-71were in the shape of a multimolecular complex which was different from that of M-mEH and could not be detected by IV–*V.

Discussion

In this study, we demonstrate that mEH in some cancerous cells takes a different shape from that of the membrane-bound form of mEH and is released to the culture medium. To analyze the antigenic structure of mEH, we developed monoclonal antibodies that recognize different parts of the mEH molecule. When we tested sera from the immunized mice by ELISA using mEH fragments as the antigens, we found that the antibody against the C-terminal half (aa 244–455) was produced only after the third immunization, while the antibody against the N-terminus (aa 1–243) appeared after the first immunization, indicating that the C-terminal half is less immunogenic than the N-terminus. We developed the monoclonal antibody 6E3 against the epitope in the C-terminal half (aa 327–353) (type IV epitope) by hyperimmunizing mice with the purified mEH. In addition, we could obtain at least four kinds of monoclonal antibodies which recognize the N-terminus or the conformational epitopes (Tables 3, 5).

To obtain antibodies against the linear epitopes of mEH, we used L-mEH for immunization. L-mEH was prepared by preparative SDS-PAGE and does not react with the antibodies against conformational epitopes as shown by ELISA (Fig. 2). However, the antibodies from 26 out of 64 hybridoma colonies reacted only with the S-mEH but not with any of F-mEH 1 to 4. From these 26 hybridomas, 2G2 and 7B11 were obtained after limiting dilution, grouped as type V and shown to recognize conformational epitopes (Fig. 2). Therefore, it seems that L-mEH regained conformational epitopes after being injected into mice. The S-mEH, which was purified after solubilization with Triton X-100 and used for screening of hybridomas, did not react with either of the type V antibodies nor anti-AN antibodies just after purification, but during storage at 4 °C, it gained the reactivity with these antibodies (data not shown). These findings are further supported by the fact that the purified mEH exists as high molecular weight aggregates (~600 kDa) in the absence of SDS (DuBois et al., 1979; Lu et al., 1975). In addition, all of the 12 monoclonal antibodies raised against AN antigen (Akatsuka et al., 1986b) were found to recognize conformational epitopes of mEH (Akatsuka et al., 1986a), and in CBA against the AN antigen, all antibodies showed 100% inhibition to each other (unpublished). One of the anti-AN antibodies (1H9) and the type V antibody 2G2 compete with each other well in the assay against the M-mEH (Table 4). Taken together, it seems that mEH is prone to form a multimolecular complex with a common conformational epitope. Any of the monoclonal antibodies did not show significant inhibition of mEH catalytic activity. It is rare to find an inhibitory antibody probably because the active site of mEH is deep inside the enzyme which forms a peculiar conformation and complex.

In Western blotting of extracts from THLE-5b and Huh-1, the three antibodies (2D8, 5D8, and 8F11) reacted with a 54 kDa band in addition to the 47 kDa band, which corresponded to an entire mEH molecule (Fig. 3B), and were grouped as type I (Table 3). Since this 54 kDa band was not observed on the blots of Sf9 cells expressing mEH by infection with a recombinant baculovirus (Fig. 3A) or BHK-21 cells expressing mEH by transfection with an expression plasmid (Akatsuka et al., 2007) (data not shown), we think this is a protein distinct from mEH and was detected by a cross-reaction. A similar cross-reaction has been reported for anti-rat mEH monoclonal antibody, 25A-3 (Ananthanarayanan et al., 1988). 25A-3 recognized a 54 kDa protein which was thought to be the Na^+-independent bile acid carrier protein, but the antigen has not been molecularly identified (D. Levy, personal communication). Because mEH is thought to be a part of a multi-protein transport system on the membranes

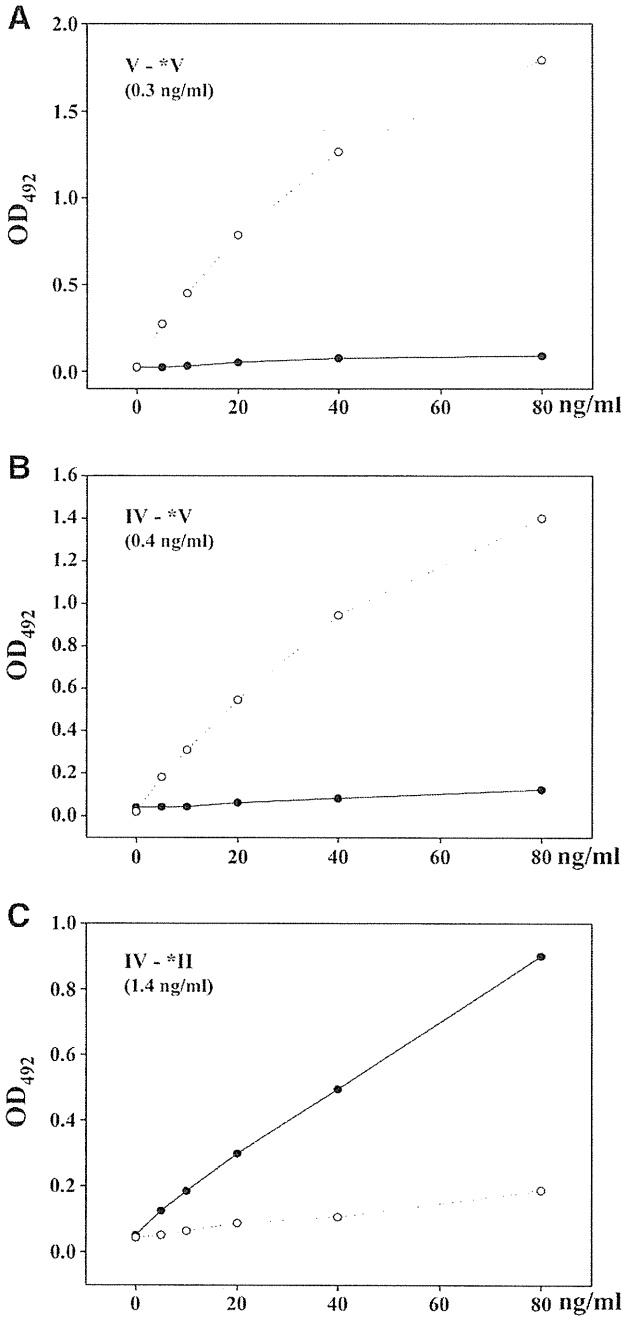

Fig. 5. Titration curves of the standard mEH antigens by antibody sandwich ELISA. Results of the three combinations of labeled (denoted by the asterisk) and unlabeled (without the asterisk) monoclonal antibodies (V–*V (A), IV–*V (B), and IV–*II (C)) are shown. ELISA plates coated with unlabeled antibodies at a concentration of 5 μg/ml were incubated with serial 2-fold dilutions of M-mEH (-○-) or L-mEH (●). After washing, the plates were incubated with optimal dilutions of HRP-labeled antibodies and washed. The color was developed by adding *o*-phenylenediamine dihydrochloride substrate and measured at an optical density of 492 nm. Cut-off values which correspond to the mean + 5 standard deviations of buffer control are shown in parentheses.

(Ananthanarayanan et al., 1988), it is worth identifying the 54 kDa protein in human cells recognized by type I antibodies to explore its possible relationship to mEH.

When we tested several combinations of the antibody in the development of sandwich assay methods for mEH antigen detection, M-mEH could be detected by the combination between the type V antibody and one of the type II to V antibodies (Table 6). This indicates that M-mEH

Table 7
mEH detection in culture supernatants by RIA. mEH in the culture supernatant was assayed by RIA with the three combinations of labeled (denoted by the asterisk) and unlabeled (without the asterisk) monoclonal antibodies and the purified mEH as the standard (L-mEH for IV–*II and M-mEH for IV–*V and V–*V). Results are expressed as ng/ml and values above the cut-off are highlighted in gray. Cut-off values were 2.1 (S/N ratio) using culture media as the negative control.

	Combinations of antibodies		
Cell line	IV–*II	IV–*V	V–*V
THLE-5b	<1.8	<1.6	<1.3
Huh-7	<1.8	<1.6	<1.36
Huh-1	<1.8	<1.6	4.26
M1	<1.8	<1.6	<1.3
U87MG	<1.8	<1.6	<1.3
LN-Z308	<1.8	<1.6	<1.3
LN-71	<1.8	<1.6	7.83

expresses all of type II to V epitopes on its surface, however, it could not be detected by the combinations between the two of the type II to IV antibodies. One possible explanation is that the linear epitopes, type II to IV, are clustered in a very small area surrounded by the complex of mEH molecules with multiple type V epitopes, and once an antibody molecule binds to one of the linear epitopes, the other linear epitopes are hindered sterically from the access by another antibody molecule. On the other hand, L-mEH could be detected well by IV–*II, but the opposite combination II–*IV did not work well. In the epitope mapping study by ELISA using the antigens F-mEH 1 to 9, the type IV antibody 6E3 showed much lower reactivity to F-mEH 5 than to F-mEH 6 although F-mEH 5 contained the entire sequence of F-mEH 6 and an additional sequence on its C-terminal side (Table 2). This finding implies that the type IV epitope has the potential to be masked by the adjacent sequence located on its C-terminal side. Therefore, once the linearized mEH (L-mEH) is bound to the type II or type III antibody or to the plastic plate, it may change its conformation on the C-terminal side and type IV epitope may lose the accessibility to the antibody. This may also explain why the mEH released from Huh-1 and LN-71 to the culture medium could not be detected by the IV–*V method. The mEH in those cells may have changed its orientation on the membrane and formed a multimolecular complex with increased solubility and with the type IV epitope being masked by the adjacent sequence.

In this study, we found that mEH is released from Huh-1 and LN-71 to the culture medium and both antigens showed similar results in our analyses which demonstrated that they have a different structure from the membrane-bound form of mEH. This antigen seems to be related to the preneoplastic antigen (PNA). Okita and Farber (1975) demonstrated that there is an antigen in preneoplastic foci in rat livers that is released into the blood, which was in later studies shown to be similar if not identical to the mEH (Levin et al., 1978). In later studies, a rapid radiochemical assay for the PNA was developed for human blood and shown to be associated with liver cancer, but it was also found to be associated with several other types of liver damage (Hammock et al., 1984). The AN antigen was purified from liver of a patient infected with HCV (Tohmatsu et al., 1985). The antigen is released into the blood in the early phase of HCV infection and the antibody appears in the acute phase of hepatitis (Akatsuka et al., 1986a, 1986b, 2007). The AN antigen is composed of particles with molecular weight of more than 1500 kDa (Tohmatsu et al., 1985) and was found to be mainly composed of mEH (Akatsuka et al., 2007). However, the AN antigen was shown to be somehow different from the membrane-bound form of mEH in that the former reacted only with the antibody in sera from HCV-infected patients whereas the latter reacted with both the antibody from patients with HCV infection and that from patients with hepatitis A virus infection (Akatsuka et al., 2007). In this study, we did not analyze the AN antigen or the antigens in sera from patients with HCV

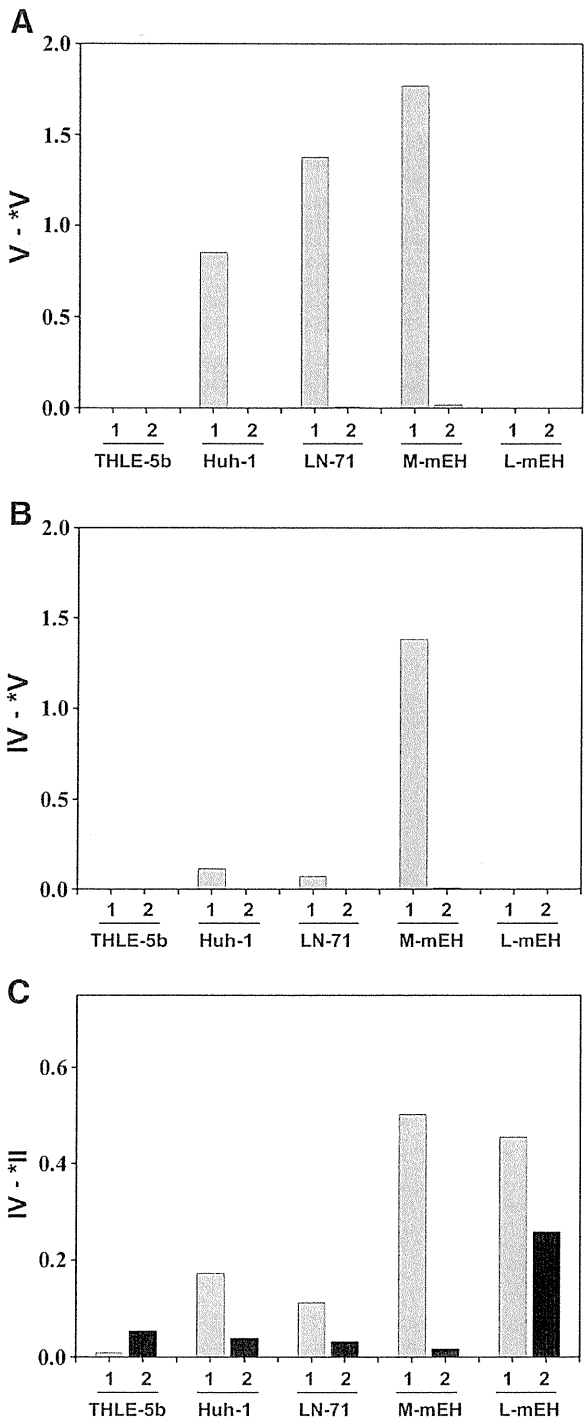

Fig. 6. Analysis of molecular sizes of mEH antigens released into the medium from THLE-5b, Huh-1 and LN-71 cultures. Culture supernatants were concentrated about 10-fold by ultrafiltration through 10 kDa cut-off membranes. Then, their aliquots and standard antigens (M-mEH and L-mEH, 80 ng/ml each) were subjected to ultrafiltration through 100 kDa cut-off membranes. The samples before (1) and after (2) ultrafiltration through 100 kDa cut-off membranes were tested by the three antigen detection ELISA methods (V-*V (A), IV-*V (B), and IV-*II (C)). In the assays by IV-*II (C), all the samples were suspended in the dilution buffer containing 0.1% SDS. The background-subtracted results are expressed by OD_{492}.

infection, but such studies will provide important information about the influence of virus infection on the expression and structure of mEH and its role in development of hepatitis.

Because mEH coordinates with other enzymes on ER membrane and plays multiple functions, disintegration of the enzymes may lead to pathological consequences such as tumorigenesis. We observed that mEH changes its location in the cells during certain virus infection in vitro, and it accompanies with the changes of mEH activities (manuscript in preparation). Further analysis of PNA-like antigens may clarify the association of mEH with the pathogenesis of some human diseases and cancer.

In summary, we have obtained monoclonal antibodies to at least five different epitopes of human mEH and developed the methods which selectively detect either the membrane-bound form or the linearized form of mEH. These methods enable us to discriminate the native form of mEH from the variant soluble form produced in some cancerous cells. The method which selectively detects the linearized form of mEH enables us to measure the mEH in any form of structure if only it has an entire sequence and linearized by SDS treatment. These tools may be valuable for elucidation of the role of mEH in various disease processes.

Conflict of interest statement

The authors declare that there are no conflicts of interest.

Acknowledgments

The authors thank Hiroe Akatsuka and Akira Takagi for technical assistance. We also thank Dr. W.E. Biddison, Dr. R. Nishikawa, and Dr. E.G. Van Meir for providing cell lines. This work was supported by a Saitama Medical University Internal Grant; a grant from Eisai Co., Ltd.; and partly supported by the National Institutes of Health National Institute of Environmental Health Sciences (R01 ES002710). BDH is a George and Judy Marcus Senior Fellow of the American Asthma Foundation.

References

Akatsuka, T., Tohmatsu, J., Abe, K., Shikata, T., Ishikawa, T., Nakajima, K., Yoshihara, N., Odaka, T., 1986a. Non-A, non-B hepatitis related AN6520 Ag is a normal cellular protein mainly expressed in liver. II. J. Med. Virol. 20, 43–56.

Akatsuka, T., Tohmatsu, J., Yoshihara, N., Katsuhara, N., Okamoto, T., Shikata, T., Odaka, T., 1986b. Detection of an antigen (AN6520) possibly related to non-A, non-B hepatitis, by monoclonal antibodies. I. J. Med. Virol. 20, 33–42.

Akatsuka, T., Kobayashi, N., Ishikawa, T., Saito, T., Shindo, M., Yamauchi, M., Kurokohchi, K., Miyazawa, H., Duan, H., Matsunaga, T., Komoda, T., Morisseau, C., Hammock, B.D., 2007. Autoantibody response to microsomal epoxide hydrolase in hepatitis C and A. J. Autoimmun. 28, 7–18.

Albertoni, M., Daub, D.M., Arden, K.C., Viars, C.S., Powell, C., Van Meir, E.G., 1998. Genetic instability leads to loss of both p53 alleles in a human glioblastoma. Oncogene 16, 321–326.

Ananthanarayanan, M., von Dippe, P., Levy, D., 1988. Identification of the hepatocyte Na+-dependent bile acid transport protein using monoclonal antibodies. J. Biol. Chem. 263, 8338–8343.

DuBois, G.C., Appella, E., Armstrong, R., Levin, W., Lu, A.Y., Jerina, D.M., 1979. Hepatic microsomal epoxide hydrase. Chemical evidence for a single polypeptide chain. J. Biol. Chem. 254, 6240–6243.

Gill, S.S., Wie, S.I., Guenthner, T.M., Oesch, F., Hammock, B.D., 1982. Rapid and sensitive enzyme-linked immunosorbent assay for the microsomal epoxide hydrolase. Carcinogenesis 3, 1307–1310.

Gill, S.S., Ota, K., Ruebner, B., Hammock, B.D., 1983. Microsomal and cytosolic epoxide hydrolase in rhesus monkey liver, and in normal and neoplastic human liver. Life Sci. 32, 2693–2700.

Hammock, B.D., Loury, D.N., Moody, D.E., Ruebner, B., Baselt, R., Milam, K.M., Volberding, P., Ketterman, A., Talcott, R., 1984. A methodology for the analysis of the preneoplastic antigen. Carcinogenesis 5, 1467–1473.

Holder, J., Yagi, H., Dansette, P., Jerina, D.M., Levin, W., Lu, A.Y.H., Conney, A.H., 1974. Effects of inducers and epoxide hydrolase on the metabolism of benzo[a]pyrene by liver microsomes and a reconstituted system: analysis by high pressure liquid chromatography. Proc. Natl. Acad. Sci. U. S. A. 71, 4356–4360.

Huh, N., Nemoto, N., Utakoji, T., 1982. Metabolic activation of benzo[a]pyrene, aflatoxin B1, and dimethylnitrosamine by a human hepatoma cell line. Mutat. Res. 94, 339–348.

Ishii, N., Maier, D., Merlo, A., Tada, M., Sawamura, Y., Diserens, A.C., Van Meir, E.G., 1999. Frequent co-alterations of TP53, p16/CDKN2A, p14ARF, PTEN tumor suppressor genes in human glioma cell lines. Brain Pathol. 9, 469–479.

Ishii, Y., Takeda, S., Yamada, H., Oguri, K., 2005. Functional protein–protein interaction of drug metabolizing enzymes. Front. Biosci. 10, 887–895.

Kessler, R., Hamou, M.-F., Albertoni, M., de Tribolet, N., Arand, M., Van Meir, E.G., 2000. Identification of the putative brain tumor antigen BF7/GE2 as the (de)toxifying enzyme microsomal epoxide hydrolase. Cancer Res. 60, 1403–1409.

Lechner, J.F., Smoot, D.T., Pfeifer, A.M., Tokiwa, T., Harris, C.C., 1991. A non-tumorigenic human liver epithelial cell culture model for chemical and biological carcinogenesis investigations. In: Rhim, J.S., Drifschlo, A. (Eds.), Neoplastic Transformation in Human Cell Systems. Humana Press, New York, pp. 307–321.

Levin, W., Lu, A.Y.H., Thomas, P.E., Ryan, D., Kizer, D.E., Griffin, M.J., 1978. Identification of epoxide hydrolase as the preneoplastic antigen in rat liver hyperplastic nodules. Proc. Natl. Acad. Sci. U. S. A. 75, 3240–3243.

Lu, A.Y.H., Ryan, D., Jerina, D.M., Daly, J.W., Levin, W., 1975. Liver microsomal epoxide hydrase. J. Biol. Chem. 250, 8283–8288.

Maekawa, K., Itoda, M., Hanioka, N., Saito, Y., Murayama, N., Nakajima, O., Soyama, A., Ishida, S., Ozawa, S., Ando, M., Sawada, J., 2003. Non-synonymous single nucleotide alterations in the microsomal epoxide hydrolase gene and their functional effects. Xenobiotica 33, 277–287.

Mcconahey, P.J., Dixon, F.J., 1966. A method of trace iodination of proteins for immunologic studies. Int. Arch. Allergy Appl. Immunol. 29, 185–189.

McGlynn, K.A., Rosvold, E.A., Lustbader, E.D., Hu, Y., Clapper, M.L., Zhou, T., Wild, C.P., Xia, X.-L., Baffoe-Bonnie, A., Ofori-Adjei, D., Chen, G.-C., London, W.T., Shen, F.-M., Buetow, K.H., 1995. Susceptibility to hepatocellular carcinoma is associated with genetic variation in the enzyme detoxication of aflatoxin B1. Proc. Natl. Acad. Sci. U. S. A. 92, 2384–2387.

Morisseau, C., Newman, J.W., Dowdy, D.L., Goodrow, M.H., Hammock, B.D., 2001. Inhibition of microsomal epoxide hydrolases by ureas, amides, and amines. Chem. Res. Toxicol. 14, 409–415.

Nakabayashi, H., Taketa, K., Miyano, K., Yamane, T., Sato, J., 1982. Growth of human hepatoma cells lines with differentiated functions in chemically defined medium. Cancer Res. 42, 3858–3863.

Newman, J.W., Morisseau, C., Hammock, B.D., 2005. Epoxide hydrolases: their roles and interactions with lipid metabolism. Prog. Lipid Res. 44, 1–51.

Okita, K., Farber, E., 1975. An antigen common to preneoplastic hepatocyte populations and to liver cancer induced by N-2-fluorenyl-acetamide, ethionine, or other hepatocarcinogens. Gann Monogr. Cancer Res. 17, 283–299.

Park, J.Y., Chen, L., Wadhwa, N., Tockman, M.S., 2005. Polymorphisms for microsomal epoxide hydrolase and genetic susceptibility to COPD. Int. J. Mol. Med. 15, 443–448.

Royer-Pokora, B., Peterson, W.D., Haseltine, W.A., 1984. Biological and biochemical characterization of an SV40-transformed xeroderma pigmentosum cell line. Exp. Cell Res. 151, 408–420.

Smith, C.A., Harrison, D.J., 1997. Association between polymorphism in gene for microsomal epoxide hydrolase and susceptibility to emphysema. Lancet 350, 630–633.

Sonzogni, L., Silvestri, L., De Silvestri, A., Gritti, C., Foti, L., Zavaglia, C., Bottelli, R., Mondelli, M.U., Civardi, E., Silini, E.M., 2002. Polymorphisms of microsomal epoxide hydrolase gene and severity of HCV-related liver disease. Hepatology 36, 195–201.

Stone, M.R., Nowinski, R.C., 1980. Topological mapping of murine leukemia virus proteins by competition-binding assays with monoclonal antibodies. Virology 100, 370–381.

Taura, K., Yamada, H., Naito, E., Ariyoshi, N., Mori, M., Oguri, K., 2002. Activation of microsomal epoxide hydrolase by interaction with cytochromes P450: kinetic analysis of the association and substrate-specific activation of epoxide hydrolase function. Arch. Biochem. Biophys. 402, 275–280.

Tohmatsu, J., Morimoto, T., Katsuhara, N., Abe, K., Shikata, T., 1985. AN6520 Ag: an antigen purified from liver with non-A, non-B hepatitis. J. Med. Virol. 15, 357–371.

von Dippe, P., Zhu, Q.S., Levy, D., 2003. Cell surface expression and bile acid transport function of one topological form of m-epoxide hydrolase. Biochem. Biophys. Res. Commun. 309, 804–809.

Zhu, Q.S., von Dippe, P., Xing, W., Levy, D., 1999. Membrane topology and cell surface targeting of microsomal epoxide hydrolase. J. Biol. Chem. 274, 27898–27904.

Available online at www.sciencedirect.com
ScienceDirect
Current Opinion in Virology

Lipoprotein component associated with hepatitis C virus is essential for virus infectivity

Yuko Shimizu[1,3], Takayuki Hishiki[1,3], Saneyuki Ujino[1], Kazuo Sugiyama[2], Kenji Funami[1] and Kunitada Shimotohno[1]

Many chronic hepatitis patients with hepatitis C virus (HCV) are observed to have a degree of steatosis which is a factor in the progression of liver diseases. Transgenic mice expressing HCV core protein develop liver steatosis before the onset of hepatocellular carcinoma, suggesting active involvement of HCV in the de-regulation of lipid metabolism in host cells. However, the role of lipid metabolism in HCV life cycle has not been fully understood until the establishment of *in vitro* HCV infection and replication system.In this review we focus on HCV production with regard to modification of lipid metabolism observed in an *in vitro* HCV infection and replication system. The importance of lipid droplet to HCV production has been recognized, possibly at the stage of virus assembly, although the precise mechanism of lipid droplet for virus production remains elusive. Association of lipoprotein with HCV in circulating blood in chronic hepatitis C patients is observed. In fact, HCV released from culture medium is also associated with lipoprotein. The fact that treatment of HCV fraction with lipoprotein lipase (LPL) abolished infectivity indicates the essential role of lipoprotein's association with virus particle in the virus life cycle. In particular, apolipoprotein E (ApoE), a component of lipoprotein associated with HCV plays a pivotal role in HCV infectivity by functioning as a virus ligand to lipoprotein receptor that also functions as HCV receptor. These results strongly suggest the direct involvement of lipid metabolism in the regulation of the HCV life cycle.

Addresses
[1] Research Institute, Chiba Institute of Technology, Tsudanuma, Narashino, Chiba 275-0016, Japan
[2] Center for Integrated Medical Research, Keio University, Shinjuku-ku, Shinanomachi 35, Tokyo 160-8582, Japan

Corresponding author: Shimotohno, Kunitada (kunitada.shimotono@it-chiba.ac.jp)
[3] These authors contributed equally.

Current Opinion in Virology 2011, **1**:19–26

This review comes from a themed issue on
Virus Entry
Edited by François-Loïc Cosset and Urs Greber

Available online 12th June 2011

1879-6257/$ – see front matter

DOI 10.1016/j.coviro.2011.05.017

Introduction

Infection with hepatitis C virus (HCV), which persists with a rate of up to 80% and is difficult to eliminate, is estimated to occur in about 3% of the world population [1]. HCV infection frequently causes chronic hepatitis, which often leads to the development of liver cirrhosis and hepatocellular carcinoma after a long latency period [2]. The combined therapy of ribavirin and interferon is currently a major treatment to infected patients, although half of them have experienced the benefit of this treatment along with a severe side effect. Therefore, clarification of the underlying molecular mechanism of HCV life cycle is necessary for the development of a new effective therapy.

The progression of liver disease in patients with HCV is thought to result from a persistent inflammation accompanied by periportal necrosis and fibrosis [3]. Many chronic hepatitis patients with HCV, but not with HBV, are also noted to have a degree of steatosis by the examination of their liver biopsies [4]. Hepatic steatosis is defined as excessive lipid accumulation/infiltration within the hepatocyte, and has recently been recognized as an important cause for cirrhosis [5]. It seems likely that hepatic steatosis in chronic hepatitis C patients is somehow related to HCV infection and its replication. Furthermore, the combination of steatosis and the presence of HCV has been associated with a more rapid progression of fibrosis. Although the precise mechanism of how HCV infection results in the accumulation of excessive lipid levels and causes hepatocyte steatosis remains elusive, increasing evidence strongly suggests that HCV-encoded protein(s) plays some roles in this process.

HCV, which belongs to the family *Flaviviridae*, has a 9.6-kb positive single strand of RNA as a genome. The HCV RNA is translated into a precursor polyprotein that is processed concertedly with translation, or after the translation by cleavage with cellular and viral proteases to produce about 10 viral proteins, structural proteins (core, E1, and E2), and nonstructural proteins (p7, NS2, NS3, NS4A, NS4B, NS5A, and NS5B). With the help of nonstructural proteins, viral replication occurs in the endoplasmic reticulum (ER) membranous structure. In this review, we discuss the effect of HCV infection on host lipid metabolism and transfer, as well as the early event of virus entry required for HCV life cycle.

Regulation of lipid metabolism by HCV proteins

Expression of HCV core as well as the complete HCV genome in some transgenic mice induces steatosis [6,7]. It is notable to observe the association of HCV core with the

surface of lipid droplet as well as apolipoprotein AII *in vitro* [8,9]. Interaction of core with lipid droplet was molecularly dissected using core mutants, and as a result the responsive region as well as structure of core was revealed [10,11••,12•]. Moreover, it has been shown that the core has a negative effect on the microsomal triglyceride transfer protein (MTP) activity [13]. Besides the HCV core, the presence of subgenomic replicon that lacks core expression has also been found to disturb MTP activity in the hepatocytes [14]. In this case, NS5A has been observed to interfere with MTP function [14]. As MTP is an essential chaperone for the assembly of very low-density lipoproteins (VLDL), which transfers triglyceride, phospholipids, and cholesterol from the hepatocytes, regulation of MTP is closely related to the accumulation of lipids in the hepatocytes. In fact, MTP deficiency results in large fat droplets in the hepatocytes and scattered accumulation of inflammatory cells [15]. HCV type-3 infected patients show reduced MTP activity and mRNA levels as well as high degree of steatosis [16]. So far, it is not clear whether MTP activity is directly regulated by HCV. Rather, MTP is likely to be controlled by activators (HNF1α, LRH-1, and HNF4α) and repressors (insulin and SREBP), some of which are modulated by HCV [14,17]. Reduced activity of MTP results in decreased secretion of VLDL, which seemingly leads to lipid accumulation. However, it is noteworthy that MTP activity is not completely suppressed by HCV. As will be described later, MTP activity is required for virus egress from infected cells. Collectively, these results suggest that HCV proteins alter lipid metabolism by activating lipid synthesis and modulating secretion of lipoprotein through interaction with cellular proteins, which results in accumulation and storage of lipids in cells expressing those viral proteins. However, the role of these viral proteins in modulating lipid metabolism related to HCV proliferation remains unknown until an *in vitro* HCV infection system was established.

Association of HCV with lipoproteins in the blood of HCV-infected individuals

HCV particles present in circulating serum show properties of heterogenous and lower density than those expected from its putative viral structure and can be captured by antilipoprotein antibody, which partly reflects the binding of a fraction of the virions to VLDL or low-density lipoproteins (LDLs) [18–22]. These low-density HCV-RNA-containing particles (called as lipo-viro-particle: LVP) contain core and apolipoprotein B (ApoB), and are rich in triglyceride with a diameter of >100 nm [19].

Although the physiological meaning of HCV-containing LVP in the circulating blood is not clear, it seems that HCV has either a high affinity to lipoproteins or is assembled with lipoproteins through the mechanism of lipoprotein synthesis. LVP-like structure may self-protect from the host immunological surveillance and/or increase interaction with lipoprotein receptor(s) which may act as a HCV receptor [20].

Importance of the lipid droplet in establishing a microenvironment for HCV assembly

The roles of modulation of lipid metabolism and association of HCV proteins with host factors involved in lipid metabolism for life cycle of HCV were not clear until an infectious *in vitro* HCV replication system was established [23–25].

Subcellular localization of HCV proteins in cells with replication of the infectious HCV RNA revealed association of core with ER membrane as well as lipid droplet. This finding is consistent with the previous reports that analyzed cells expressing on the core complex [11]. NS proteins, such as NS5A and NS5B, were found to be distributed around the core-coated lipid droplet as well as ER membrane. HCV envelope protein, E2, was detectable in the lipid droplet-enriched fraction isolated by density gradient centrifugation. Importantly, the lipid droplet present in the cytoplasm, detected by BODIPY 493/503 staining, was observed to be enriched in HCV genome replicating cells in a core-dependent manner. Furthermore, it was noted that the cells harboring HCV genome, which lacked core-coding region, did not accumulate the lipid droplet, indicating the importance of core function to activate cellular lipid metabolism, as suggested previously [17]. Moreover, the HCV genome encoding a mutant core, unable to associate with the lipid droplet, failed to produce virus. This suggests the importance of the association of core with the lipid droplet for virus assembly and release. The core-coated lipid droplet is surrounded by membranous components that are rich in nonstructural HCV proteins that constitute HCV replication complex. This spatial microenvironment seems to be important not only for virus assembly, but also for infectious virus production, because the HCV genomes carrying NS5A point mutations, which are not associated with the core-coated lipid droplet, reduce or inhibit the production of infectious virus despite minimal interference with the replication of the genome [11,26•]. Moreover, other NS proteins do not associate with the lipid droplet in cells bearing the NS5A-mutated HCV replicon. Thus, NS5A may have a crucial role in recruiting other NS proteins around the core-coated lipid droplet. However, how the HCV assembly takes place from such a microenvironment is still unclear.

Recent data have shown the importance of NS2 for viral morphogenesis. Molecular interactions between NS2 and other HCV proteins, such as envelope proteins (E1/E2), p7 and NS3 have been demonstrated, which suggest bridging between structural and nonstructural viral proteins and involvement in the assembly process [27–29]. NS2 accumulates in the ER-derived membranous

structures and co-localizes with the viral envelope glycoproteins and viral components of the replication complex at close proximity to the HCV core protein and lipid droplets.

Using HCV subgenome replicon cells, we have previously shown that very few HCV nonstructural protein complexes embedded in the membranous structure (referred as 'replication complex'; areas stained with dark blue color (Figure 2) are sufficient to synthesize HCV RNA present in the HCV replicon cells [30]. The level of the HCV proteins in the 'replication complex,' estimated by western blot analysis, has been found to be lower than one-tenth of the total viral proteins in the cells. The majority of the other HCV nonstructural proteins have been observed to remain associated with the ER membrane, possibly as a complex that is not protected by membranous components. As NS2 is dispensable for HCV RNA synthesis, it is likely that NS2 is not necessarily associated with the 'replication complex.' However, NS2 that is associated with envelopes and p7 has also been found to be associated with NS3 in the nonstructural protein complex that is not protected by the membrane. In this study, we refer to this complex as the 'HCV protein complex.'

Involvement of lipoproteins in HCV assembly and its infectivity

Lipoprotein is a biochemical particle consisting of apolipoproteins, triglyceride, cholesterol, and phospholipids, and transfers lipids through the bloodstream to the tissues. Liver, an endogenous source of lipoproteins, synthesizes VLDL using MTP. Lipoprotein lipase (LPL) hydrolyzes VLDL to supply lipids to the tissues, and converts VLDL into intermediate density lipoprotein (IDL). Hepatic triglyceride lipase (HTGL) hydrolyzes IDL to LDL.

ApoB is a main component of VLDL produced in the hepatocytes. Several groups have asserted the requirement of ApoB for HCV production [31•,32•,33•]. Huang *et al.* [31•] demonstrated that ApoB reduction by MTP inhibitor or a siRNA against ApoB led to decreased infectious HCV production. Gastaminza *et al.* [32•] reported similar results. Icard *et al.* [33•] showed that the release of HCV envelopes depended on the secretion of ApoB. Another study [34•] showed negative data for the requirement of ApoB, in which the authors described that apolipoprotein E (ApoE) rather than ApoB is important for HCV production and infectivity. Thus, ApoB requirement for virus production is still unclear.

ApoE, a component of lipoproteins, has attracted much attention as an important factor for HCV infectivity, because it has been shown that knockdown of ApoE could reduce HCV infectivity at a higher degree than the knockdown of ApoB, apolipoprotein A1 (ApoA1), and ApoC1 ([35••,36••], and data not shown). ApoE has three major isoforms (ApoE2, ApoE3, and ApoE4) differing by amino acid substitution at one or two sites (residues 130 and 176), which have different effects on lipid and neuronal homeostasis. ApoE3 is the most common isoform with no report of association with disease. ApoE2 has lower affinity for the low-density lipoprotein receptor (LDLR) and is a major risk factor for type III hyperlipoproteinemia, while ApoE4 is the major risk factor for Alzheimer's disease. Since ApoE not only functions as a ligand for LDLR and scavenger receptor class B type 1 (SR-B1), but also is associated with HCV, the effect of ApoE associated with HCV on the interaction of these lipoprotein receptors was examined by measuring the infectivity in naïve cells. Rescue of ApoE with ApoE3 ectopic expression in ApoE-knockdown cells recovered HCV infectivity, whereas ectopic ApoE2 expression did not. This result strongly indicates that ApoE, in particular some isoforms of ApoE, is necessary for HCV infectivity. ApoA1, a component of chylomicron, LDL, and high-density lipoprotein (HDL), is also important for HCV production, but is found to be less effective than ApoE ([37] and unpublished data). Taken together, HCV is seemingly produced as a hybrid of HCV and lipoproteins. While VLDL is a main lipoprotein secreted from normal hepatocytes, HCV may modulate the production of lipoproteins in the host cells to make the original lipoproteins more effective/appropriate for viral replication and persistence.

To further strengthen the involvement of lipoproteins in HCV infectivity, we evaluated HCV as a substrate of LPL [38•]. LPL treatment significantly suppressed HCV infectivity and increased the buoyant density of HCV (Figure 1a; modified from Ref. [38•]). This indicates that LPL hydrolyzes lipoproteins fused with HCV to result in decreased HCV infectivity. In accordance with the change in the buoyant density, the amount of ApoE associated with HCV decreased. As the HCV-bearing supernatant used in this study contained endogenous HTGL from the hepatocytes, these effects might result from HTGL in addition to LPL. Thus, we consider that detachment of ApoE from the HCV particle led to reduced HCV entry.

Relation between HCV particle size and infectivity

Ultracentrifugation of HCV in a gradient of iodixanol has revealed the discrepancy in buoyant density between the major virus peak and the virus with infectivity; the latter showed lower buoyant density than the former. However, the underlying physicochemical differences between noninfectious and infectious viruses still remain elusive. Thus, we tried to characterize the infectious virus from a different perspective. To evaluate the relationship between virus size and infectivity, the virus was analyzed by gel filtration chromatography (Shimizu *et al.*, unpublished

Figure 1

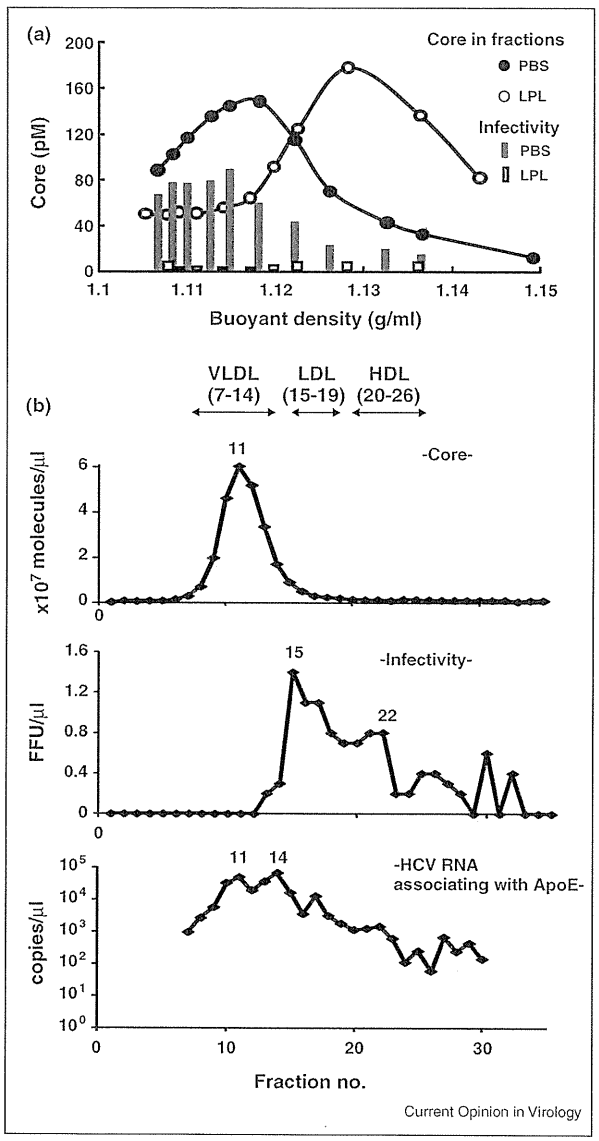

Relationship between physicochemical properties and infectivity of HCV. **(a)** LPL treatment shifts HCV to higher buoyant density and reduces HCV infectivity. The HCV (JFH1)-bearing culture medium was treated with PBS or LPL (500 μg/ml) for 1 hour at 37 °C and ultracentrifuged through iodixanol gradients. Thirty fractions were collected for analyzing the amount of core by ELISA. Culture medium from HuH7.5 cells inoculated with aliquots of each fraction was subjected to Core ELISA for infectivity. **(b)** Size distribution of HCV, infectious HCV, and HCV associated with ApoE. The HCV (JFH1)-bearing culture medium was subjected to gel filtration chromatography. The sample was eluted with 0.05 mol/l Tris-buffered acetate (pH 8.0) containing 0.3 mol/l sodium acetate, 0.05% sodium azide, and 0.005% Brij-35. A total of 50 fractions collected were analyzed for core, infectivity, and HCV RNA associated with ApoE. The representative fractions from 1 to 35 (core and infectivity) and from 7 to 30 (HCV RNA associated with ApoE) are shown. Elution of VLDL, LDL, and HDL was found in fractions 7–14, 15–19, and 20–26, respectively.

data). HCV released from infected HuH7.5 cells was applied to in-tandem-connected columns (300 mm × 7.8 mm) of TSKgel LipopropakXL resin (Tosoh, Tokyo). The eluent from the column was continuously separated into a total of 50 fractions. Then, each fraction was analyzed for core, HCV RNA, infectivity, ApoE, and E2. The major peak of the core was in fraction (frac.) 11 (Figure 1b). The HCV RNA peak corresponded to the core peak. E2 associated with the viral particle, analyzed by immunoprecipitation (IP) using anti-E2 antibody followed by RT-PCR for HCV RNA, was also in this fraction. This suggests that HCV eluted to frac. 11 retained the virus-like structure. However, importantly, HCV in frac. 11 did not have infectivity. The HCV fraction associated with infectivity showed multiple peaks ranging from frac. 15 to 22. Furthermore, frac. 15 demonstrated highest infectivity among all the fractions, and there was no linear correlation between the virus size and infectivity.

To determine whether the lack of ApoE is implicated in undetectable infectivity of HCV in frac. 11, we quantified HCV RNA associated with ApoE in each fraction by IP using anti-ApoE antibody, followed by RT-PCR. The HCV RNA associated with ApoE was detected from fractions irrespective of HCV infectivity (Figure 1b). This indicates that the association with ApoE is a necessary factor, but not sufficient for HCV infectivity.

Model of HCV budding into ER lumen

By taking these observations on HCV assembly into consideration, we drew the model of HCV assembly process and virus egress to ER lumen (Figure 2). The microenvironment of membranous structure of the core-coated lipid droplet has been found to play important roles in virus assembly [11••]. However, there is no proof to show a direct interaction of the core-coated lipid droplet with other HCV proteins. We presume that the core-coated lipid droplet may be localized at the vicinity of the 'HCV protein complex' enriched ER membrane, and that the triglyceride and cholesterol of the lipid droplet are reversely transferred to the inside of the bilayer of the ER membrane to where the core gets accumulated (Figure 2, stage a) [11••]. Core protein is not only enriched on the lipid droplet, but also visible on the ER by confocal microscopy [11••]. The presence of membranous web structure in the HCV genome replicating cells suggests dynamic alteration of the ER membrane structure [39]. Formation of the membranous web may include production of the 'replication complex' as well as dynamic alteration of ER membranous structure surrounding the core-coated lipid droplet, to make close association of 'replication complex' with core-enriched putative budding site of the viral particle (Figure 2, stage b). HCV protein complexes may gather each other to establish a compartment to constitute the 'replication complex' and putative virus precursor, so that the HCV

Figure 2

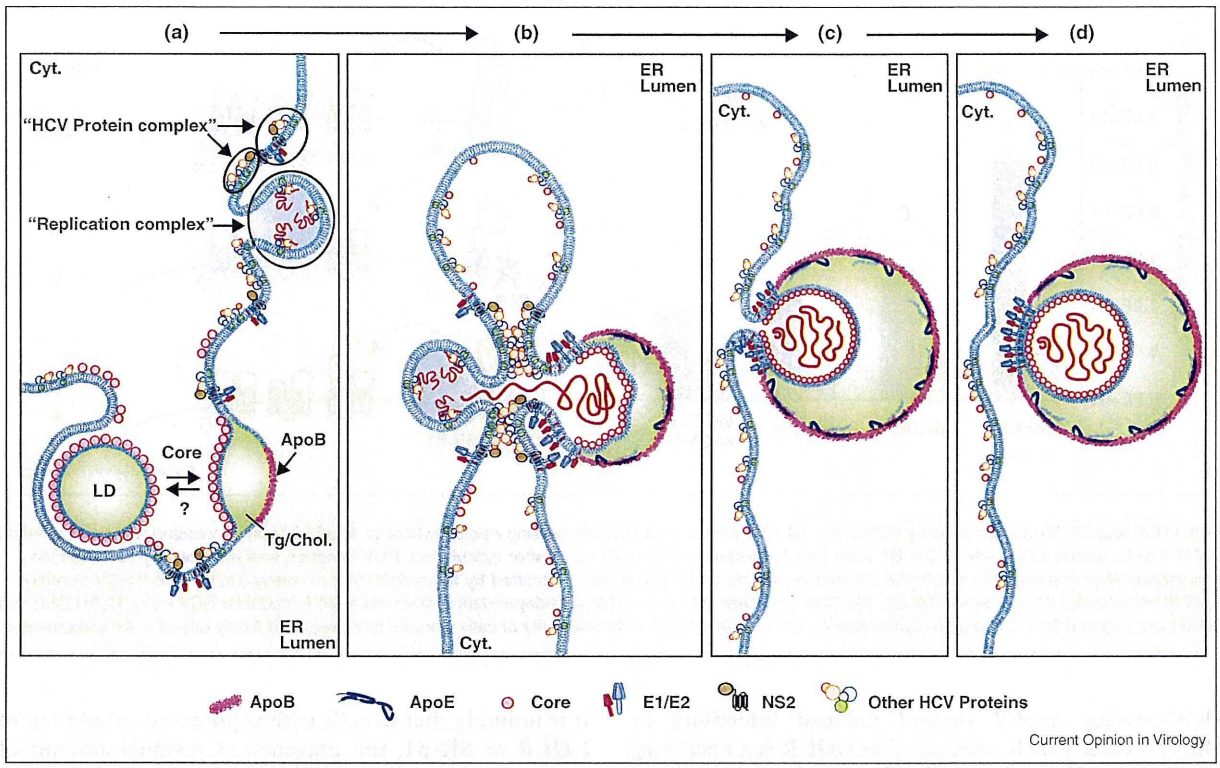

A model of virus egress to ER lumen. Stage **(a)**: Accumulation of triglyceride and cholesterol in the inside of the ER bilayer membrane enhances core association with the cytoplasmic monolayer membrane. These lipids may be reversely transferred from the core-coated lipid droplet or may be present in the inside of the ER bilayer membrane *ab origine*. On the membrane of ER, 'replication complex' as well as 'HCV protein complex' exists. Stage **(b)**: Distortion of the ER membrane, which seems to be driven by HCV protein complexes, makes the "Replication complex" location in the vicinity of the core-coated lipid-rich ER membrane, where HCV RNA secreted from the "replication complex" is exported to the putative virus budding site to establish a nascent HCV nucleocapsid. Simultaneously, ApoB and MTP function to synthesize lipoprotein-like structure surrounding the viral particle. Stages **(c)** and **(d)**: Progressing images of Stage B until egress of the virus/lipoprotein complex into ER lumen.

genome synthesized in the 'replication complex' is exported to the putative precursor of the viral particle to make a nascent HCV nucleocapsid. Simultaneously, lipoprotein formation proceeds with the help of MTP and ApoB, and buds into the ER lumen (Figure 2, stages c and d). It is still not clear at which stage of the virus assembly, other apolipoproteins, such as ApoA1 and ApoE, are incorporated into the virus/lipoprotein complex. However, NS5A may play some roles in incorporating ApoE into virus/lipoprotein complex during the process of virus assembly, because ApoE associates with NS5A [40].

Both LDLR and SR-B1 are likely to be recognized by HCV for adsorption into naïve cells for entry

Several cell-surface molecules, such as CD81, Claudin, Occludin, SR-B1, LDLR, and glycosaminoglycan heparan sulfate (HS) function as receptors for HCV infection [41,42,43•,44••,45]. Suppressed expression of any of these molecules in naïve HuH7.5 cells reduces or inhibits HCV infection [44••,46], indicating the necessity of concerted action by these molecules for entry and full establishment of HCV infection. However, hierarchical order of actions by these molecules in the process of HCV entry remains elusive.

SR-B1 is expressed in many cells, but is mainly expressed in the liver and steroidogenic tissues. SR-B1 recognizes various types of lipoproteins that include HDL, LDL, and VLDL, as well as modified lipoproteins, such as oxidized and acetylated LDL. In addition, SR-B1 is shown to be associated with the soluble recombinant HCV E2 glycoprotein [47]. LDLR, expressed in many tissues including liver, is a cell-surface receptor that recognizes ApoB in LDL and ApoE in IDL and VLDL.

It is still controversial whether LDLR or SR-B1 is used as an entry receptor by HCV [42,44••]. To address this problem, infectivity was analyzed on HCV bearing a different ApoE isoform [36••]. As described earlier,

Figure 3

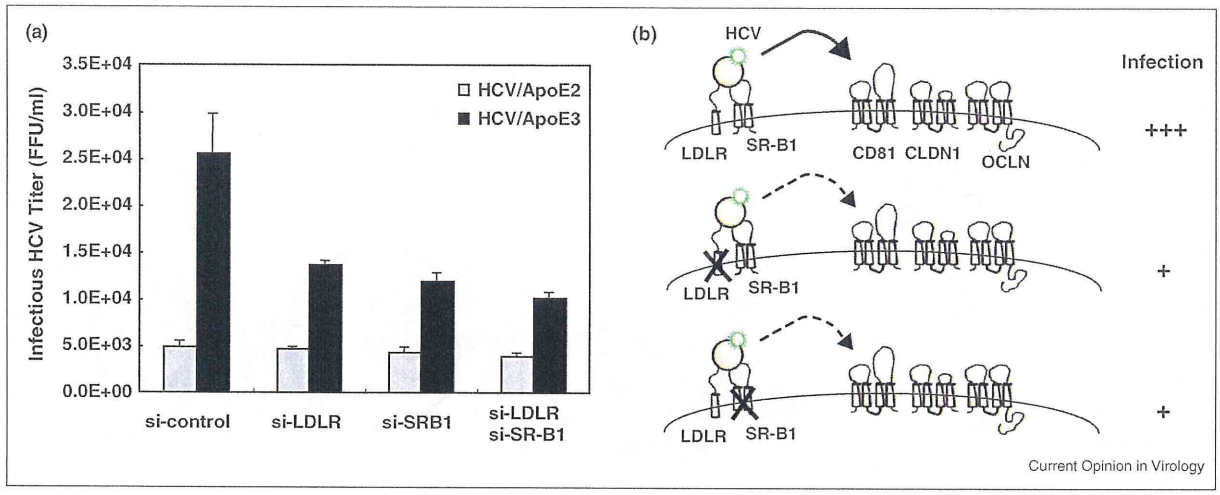

Both LDLR and SR-B1 are required for HCV entry. **(a)** HCV produced from cells bearing ApoE2 (white) or ApoE3 (black) expression was used to infect HuH7.5 cells, whose LDLR and/or SR-B1 were knocked down. Forty-eight hours after inoculation, HCV infection was analyzed by fluorescence microscopy after staining with anti-NS5A antibodies. Infectious HCV titer was quantified by focus-forming unit assay. HCV/ApoE2: HCV-bearing ApoE2; HCV/ApoE3: HCV-bearing ApoE3. The data represent the means of three independent experiments. **(b)** A model for HCV entry. Both LDLR and SR-B1 are required for HCV to gain high infectivity. On the other hand, HCV infectivity of cells is found to be reduced if only one of them is expressed.

HCV-bearing ApoE2 showed reduced infectivity in HuH7.5 cells, which indicates that LDLR is a necessary receptor for HCV infection [36••]. Further, infectivity of HCV to LDLR or SR-B1 knockdown cells was examined. Infectivity of HCV-bearing ApoE3 was reduced almost to the same level in LDLR or SR-B1 knockdown cells. With the expectation of additive reduction in infectivity in the cells with double knockdown of LDLR and SR-B1, infection in the double knockdown cells was analyzed [36••]. Unexpectedly, cells with suppressed expression of both the receptors did not show additive reduction in infectivity (Figure 3a). The level of infection of HCV-bearing ApoE2 to cells with suppressed expression of LDLR, SR-B1, or LDLR/SR-B1 was almost the same as that of the si-control transduced HuH7.5 cells (Figure 3a).

With regard to LDLR knockdown cells, the result was as expected, because ApoE2 has been found to have low affinity to LDLR. However, with regard to SR-B1 knockdown cells, we expected further reduction in HCV infection than that observed in si-control cells, because there was no significant difference in the association of ApoE2 and ApoE3 with SR-B1 [48]. Infectivity analysis using antibodies against LDLR/SR-B1 showed similar result as that observed in infectivity to LDLR or SR-B1 knockdown cells. From these results, we presume that HCV requires both LDLR and SR-B1 for infection and lack of either of the proteins suppresses HCV infectivity, as shown in Figure 3b. However, it is not known why the interaction of HCV with these two molecules results in high infectivity.

It is unlikely that in cells with suppressed expression of LDLR or SR-B1, the presence of residual amount of these proteins could establish infectivity of HCV-bearing ApoE3, because >90% reduction of these proteins in the knockdown cells has been confirmed [36]. However, this suggests the presence of another receptor through which ApoE-associated HCV could interact. To isolate a new candidate for HCV receptor(s), we focused our attention on lipoprotein receptor(s) in HuH7.5 cells. High expression of LRP1 and LRP8 was observed in this cell line among the candidates. However, knockdown of these genes in the cells did not reduce their susceptibility to HCV infection. Thus, it is likely that an unidentified protein in the HuH7.5 cells could play a role.

Conclusion

Patients with chronic hepatitis C often develop steatohepatitis. However, the reason why HCV-infected individuals cause abnormal lipid metabolism remains elusive. Recently it is suggested that HCV diverts lipid metabolism of host cells to establish its own proliferative machinery. This includes accumulation of lipid droplets to establish the microenvironment for virus assembly as modeled in this paper, and modification of lipid transfer for virus egress. Association of lipoprotein with HCV was biochemically demonstrated. Moreover, lipoprotein component(s) such as ApoE associated with virus is required for viral entry and may determine cell tropism. Further elucidation of the entire mechanism of HCV infection as well as identification of the host factors involved in this

process may contribute to more effective therapies for liver diseases caused by HCV infection.

Acknowledgements

We are grateful to Drs C. Rice and T. Wakita for HuH7.5 and JFH1 cells, respectively, and Dr J. McCubrey, East Carolina University, for comments on this manuscript. This work was supported by Grants-in-Aid for Scientific Research from the Ministry of Health, Labor, and Welfare of Japan and from the Ministry of Education, Culture, Sports, Science, and Technology.

References and recommended reading

Papers of particular interest, published within the period of review, have been highlighted as:

- • of special interest
- •• of outstanding interest

1. World Health Organization: **Hepatitis C: global prevalence**. *Wkly Epidemiol Rec* 2000, **75**:18-19.

2. Liang TJ, Jeffers LJ, Reddy KR, de Medina M, Parker IT, Cheinquer H, Idrovo V, Rabassa A, Schiff ER: **Viral pathogenesis of hepatocellular carcinoma in the United States**. *Hepatology* 1993, **18**:1326-1333.

3. Yoon EJ, Hu K-Q: **Hepatitis C virus infection and hepatic steatosis**. *Int J Med Sci* 2006, **3**:53-56.

4. Goodman ZD, Ishak KG: **Histopathology of hepatitis C virus infection**. *Semin Liver Dis* 1995, **15**:70-91.

5. Brunt EM: **Nonalcoholic steatohepatitis: definition and pathology**. *Semin Liver Dis* 2001, **21**:3-16.

6. Moriya K, Fujie H, Shintani Y, Yotsuyanagi H, Tsutsumi T, Ishibashi K, Matsuura Y, Kimura S, Miyamura T, Koike K: **The core protein of hepatitis C virus induces hepatocellular carcinoma in transgenic mice**. *Nat Med* 1998, **4**:1065-1070.

7. Lerat H, Honda M, Beard MR, Loesch K, Sun J, Yang Y, Okuda M, Gosert R, Xiao SY, Weinman SA *et al.*: **Steatosis and liver cancer in transgenic mice expressing the structural and nonstructural proteins of hepatitis C virus**. *Gastroenterology* 2002, **122**:352-365.

8. Barba G, Harper F, Harada T, Kohara M, Goulinet S, Matsuura Y, Eder G, Schaff Z, Chapman M, Miyamura T *et al.*: **Hepatitis C virus core protein shows a cytoplasmic localization and associates to cellular lipid storage droplets**. *Proc Natl Acad Sci U S A* 1997, **94**:1200-1205.

9. Sabile A, Perlemuter G, Bonbo F, Kohara K, Demaugre F, Matsuura Y, Brechot C, Barba G: **Hepatitis C virus core protein binds to apolipoprotein A11 and its secretion is modulated by fibrates**. *Hepatology* 1999, **4**:1064-1076.

10. Targett-Adams P, Hope G, Boulant S, McLauchlan J: **Maturation of hepatitis C virus core protein by signal peptide peptidase is required for virus production**. *J Biol Chem* 2008, **283**:16850-16859.

11. •• Miyanari Y, Atsuzawa K, Usuda N, Watashi K, Hishiki T, Zayas M, Bartenschlager R, Wakita T, Hijikata M, Shimotohno K: **The lipid droplet is an important organelle for hepatitis C virus production**. *Nat Cell Biol* 2007, **9**:1089-1097.
Increased lipid droplet by HCV infection was shown to be important for virus production.

12. • Shavinskaya A, Boulant S, Penin F, McLauchlan J, Bartenschlager R: **The lipid droplet binding domain of hepatitis C virus core protein is a major determinant for efficient virus assembly**. *J Biol Chem* 2007, **282**:37158-37169.
Association of HCV core with the lipid droplet requires HCV production.

13. Perlemuter G, Sabile A, Letteron P, Vona G, Topilco A, Chrétien Y, Koike K, Pessayre D, Chapman J, Barba G *et al.*: **Hepatitis C virus core protein inhibits microsomal triglyceride transfer protein activity and very low density lipoprotein secretion: a model of viral-related steatosis**. *FASEB J* 2002, **16**:185-194.

14. Domitrovich AM, Femlee DJ, Siddiqui A: **Hepatitis C virus nonstructural proteins inhibit apolipoprotein B100 secretion**. *J Biol Chem* 2005, **280**:39802-39808.

15. Partin JS, Partin JC, Schubert WK, McAdams AJ: **Liver ultrastructure in abetalipoproteinemia: evolution of micronodular cirrhosis**. *Gastroenterology* 1974, **67**:107-118.

16. Mirandola S, Realdon S, Iqbal J, Gerotto M, Dal Pero F, Bortoletto G, Marcolongo M, Vario A, Datz MM, Hussain MM *et al.*: **Liver microsomal trigriceride transfer protein is involved in hepatitis C liver steatosis**. *Gastroenterology* 2006, **130**:1661-1669.

17. Moriishi K, Mochizuki R, Moriya K, Miyamoto H, Mori Y, Abe T, Murata S, Tanaka K, Miyamura T, Suzuki T *et al.*: **Critical role of PA28gannma in hepatitis C virus-associated steatogenesis and hepatocellular carcinoma**. *Proc Natl Acad Sci U S A* 2007, **104**:1661-1666.

18. Thomssen R, Bonk S, Thiele A: **Density heterogeneities of hepatitis C virus in human sera due to the binding of β-lipoproteins and immunoglobulins**. *Med Microbiol Immunol* 1993, **182**:329-334.

19. André P, Komurian-Pradel F, Deforges S, Perret M, Berland JL, Sodoyer M, Pol S, Bréchot C, Paranhos-Baccalà G, Lotteau V: **Characterization of low- and very-low-density hepatitis C virus RNA-containing particles**. *J Virol* 2002, **76**:6919-6928.

20. Agnello V, Abel G, Elfahal M, Knight GB, Zhang QX: **Hepatitis C virus and other flaviviridae viruses enter cells via low density lipoprotein receptor**. *Proc Natl Acad Sci U S A* 1999, **96**:12766-12771.

21. Molina S, Castet V, Fournier-Wirth C, Pichard-Garcia L, Avner R, Harats D, Roitelman J, Barbaras R, Graber P, Ghersa P *et al.*: **The low-density lipoprotein receptor plays a role in the infection of primary human hepatocytes by hepatitis C virus**. *J Hepatol* 2007, **46**:411-419.

22. Thomssen R, Bonk S, Propfe C, Heermann K-H, Köchel HG, Uy A: **Association of hepatitis C virus in human sera with β-lipoprotein**. *Med Microbiol Immunol* 1992, **181**:293-300.

23. Lindenbach BD, Evans MJ, Syder AJ, Wolk B, Tellinghuisen TL, Liu CC, Maruyama T, Hynes RO, Burton DR, McKeating JA *et al.*: **Complete replication of hepatitis C virus in cell culture**. *Science* 2005, **309**:623-626.

24. Wakita T, Pietschmann T, Kato T, Date T, Miyamoto M, Zhao Z, Murthy K, Habermann A, Krausslich HG, Mizokami M *et al.*: **Production of infectious hepatitis C virus in tissue culture from a cloned viral genome**. *Nat Med* 2005, **11**:791-796.

25. Zhong J, Gastaminza P, Cheng G, Kapadia S, Kato T, Burton DR, Wieland SF, Uprichard SL, Wakita T, Chisari FV: **Robust hepatitis C virus infection in vitro**. *Proc Natl Acad Sci U S A* 2005, **102**:9294-9299.

26. • Masaki T, Suzuki R, Murakami K, Aizaki H, Ishii K, Murayama A, Date T, Matsuura Y, Miyamura T, Wakita T *et al.*: **Interaction of hepatitis C virus nonstructural protein 5A with core protein is critical for the production of infectious virus particles**. *J Virol* 2008, **82**:7964-7976.
Point mutation in the domain 3 of HCV NS5A protein abrogates production of virus particle.

27. Yi M, Ma Y, Yates J, Lemon SM: **Trans-complementation of an NS2 defect in a late step in hepatitis C virus (HCV) particle assembly and maturation**. *PLoS Pathog* 2009, **5**:e1000403.

28. Jirasko V, Montserret R, Lee JY, Gouttenoire J, Moradpour D, Penin F, Bartenschlager R: **Structural and functional studies of nonstructural protein 2 of the hepatitis C virus reveal its key role as organizer of virion assembly**. *PLoS Pathog* 2010, **6**:e1001233.

29. Ma Y, Anantpadma M, Timpe JM, Shanmugam S, Singh SM, Lemon SM, Yi M: **Hepatitis C virus NS2 protein serves as a scaffold for virus assembly by interacting with both structural and nonstructural proteins**. *J Virol* 2011, **85**:1706-1717.

30. Miyanari Y, Hijikata M, Yamaji M, Hosaka M, Takahashi H, Shimotohno K: **Hepatitis C virus non-structural proteins in the probable membranous compartment function in viral genome replication**. *J Biol Chem* 2003, **278**:50301-50308.

31. • Huang H, Sun F, Owen DM, Li W, Chen Y, Gale M Jr, Ye J: **Hepatitis C virus production by human hepatocytes**

dependent on assembly and secretion of very low-density lipoproteins. *Proc Natl Acad Sci U S A* 2007, **104**:5848-5853.
Functional association of HCV egress and VLDL has been shown.

32. Gastaminza P, Cheng G, Wieland S, Zhong J, Liao W, Chisari FV:
• **Cellular determinants of hepatitis C virus assembly, maturation, degradation, and secretion.** *J Virol* 2008, **82**:2120-2129.
See annotation to [31•].

33. Icard V, Diaz O, Scholtes C, -Cocon P, Ramière L,
• Bartenschlager C, Penin R, Lotteau F, André VP: **Secretion of hepatitis C virus envelope glycoproteins depends on assembly of apolipoprotein B positive lipoproteins.** *PLos ONE* 2009, **4**:e4223.
Association of HCV envelope protein and lipoprotein is disclosed.

34. Jing J, Luo G: **Apolipoprotein E but not B is required for the**
• **formation of infectious hepatitis C virus particles.** *J Virol* 2009, **83**:12680-12691.
Importance of apolipoprotein E rather than apolipoprotein B in infectious HCV production is described.

35. Chang K-S, Jiang J, Cai Z, Luo G: **Human apolipoprotein E is**
•• **required for infectivity and production of hepatitis C virus in cell culture.** *J Virol* 2007, **81**:13783-13793.
Apolipoprotein E plays important role in HCV infectivity.

36. Hishiki T, Shimizu Y, Tobita R, Sugiyama K, Ogawa K, Funami K,
•• Ohsaki Y, Fujimoto T, Takaku H, Wakita T *et al.*: **Infectivity of hepatitis C virus is influenced by association with apolipoprotein E isoforms.** *J Virol* 2010, **84**:12048-12057.
HCV infectivity is influenced by apolipoprotein E isoforms.

37. Mancone C, Steindler C, Santangelo L, Simonte G, Vlassi C, Longo MA, D'Offizi G, Di Giacomo C, Pucillo LP, Amicone L *et al.*: **Hepatitis C virus production requires apolipoprotein A-I and affects its association with nascent low-density lipoproteins.** *Gut* 2011, **60**:378-386.

38. Shimizu Y, Hishiki T, Sugiyama K, Ogawa K, Funami K, Kato A,
• Ohsaki Y, Fujimoto T, Takaku H, Shimotohno K: **Lipoprotein lipase and hepatic triglyceride lipase reduce the infectivity of hepatitis C virus (HCV) through their catalytic activities on HCV-associated lipoproteins.** *Virology* 2010, **407**:152-159.
Association of HCV with lipoprotein is shown by biochemical analysis.

39. Gosert R, Egger D, Lohmann V, Bartenschlager R, Blum HE, Bienz K, Moradpour D: **Identification of the hepatitis C virus RNA replication complex in Huh-7 cells harboring subgenomic replicons.** *J Virol* 2003, **77**:5487-5492.

40. Benga WJ, Krieger SE, Dimitrova M, Zeisel MB, Parnot M, Lupberger J, Hildt E, Luo G, McLauchlan J, Baumert TF *et al.*: **Apolipoprotein E interacts with hepatitis C virus nonstructural protein 5A and determines assembly of infectious particles.** *Hepatology* 2010, **51**:43-53.

41. Pileri P, Uematsu Y, Campagnoli S, Galli G, Falugi F, Petracca R, Weiner AJ, Houghton M, Rosa D, Grandi G *et al.*: **Binding of hepatitis C virus to CD81.** *Science* 1998, **282**:938-941.

42. Bartosch B, Vitelli A, Granier C, Goujon C, Dubuisson J, Pascale S, Scarselli E, Cortese R, Nicosia A, Cosset F-L: **Cell entry of hepatitis C virus requires a set of co-receptors that include the CD81 tetraspanin and the SR-B1 scavenger receptor.** *J Biol Chem* 2003, **278**:41624-41630.

43. Evans MJ, von Hahn T, Tscherne DM, Syder AJ, Panis M, Wolk B,
• Hatziioannou T, McKeating JA, Bieniasz PD, Rice CM: **Claudin-1 is a hepatitis C virus co-receptor required for a late step in entry.** *Nature* 2007, **446**:801-805.
Claudin-1 has been shown to be a receptor for HCV.

44. Owen DM, Huang H, Ye J, Gale M Jr: **Apolipoprotein E on**
•• **hepatitis C virion facilitates infection through interaction with low-density lipoprotein receptor.** *Virology* 2009, **394**:99-108.
LDLR is shown to be a receptor for HCV.

45. Barth H, Schafer C, Adah MI, Zhang F, Linhardt RJ, Toyoda H, K-Toyoda A, Toida T, van Kuppevelt TH, Depla E *et al.*: **Cellular binding of hepatitis C virus envelope glycoprotein E2 requires cell surface heparan sulfate.** *J Biol Chem* 2003, **278**:41003-41012.

46. Zeisel MB, Koutsoudakis G, Schnober EK, Haberstroh A, Blum HE, Cosset FL, Wakita T, Jaeck D, Doffoel M, Royer C *et al.*: **Scavenger receptor class B type I is a key host factor for hepatitis C virus infection required for an entry step closely linked to CD81.** *Hepatology* 2007, **46**:1722-1731.

47. Scarselli E, Ansuini H, Cerino R, Roccasecca RM, Acali S, Filocamo G, Traboni C, Nicosia A, Cortese R, Vitell A: **The human scavenger receptor class B type I is a novel candidate receptor for the hepatitis C virus.** *EMBO J* 2002, **21**:5017-5025.

48. Li X, Kan HY, Lavrentiadou S, Krieger M, Zannis V: **Reconstituted discoidal ApoE-phospholipid particles are ligands for the scavenger receptor BI.** *J Biol Chem* 2002, **277**:21149-21157.